IEEE Access
Multidisciplinary | Rapid Review | Open Access Journal

Received October 17, 2016, accepted November 20, 2016. Date of publication xxxx 00, 0000, date of current version xxxx 00, 0000.

Digital Object Identifier 10.1109/ACCESS.2016.2637568

Comprehensive Performance Analysis of Fully Cooperative Communication in WBANs

L. C. TRAN[1], (Member, IEEE), A. MERTINS[2], (Senior Member, IEEE), X. HUANG[3], (Senior Member, IEEE), AND F. SAFAEI[1], (Senior Member, IEEE)

[1]University of Wollongong, Wollongong, NSW 2522, Australia
[2]University of Lübeck, Lübeck, 23562, Germany
[3]University of Technology Sydney, Ultimo, NSW 2007, Australia

Corresponding author: L. C. Tran (lctran@uow.edu.au)

This work was supported by the Alexander von Humboldt Foundation, Germany, through the Humboldt Renewed Research Stay Fellowship under Grant 3.5-AUS/1120905 STP.

ABSTRACT While relay-based cooperative networks (widely known in the literature as cooperative communication), where relays only forward signals from the sources to the destination, have been extensively researched, fully cooperative systems have not been thoroughly examined. Unlike relay networks, in a fully cooperative network, each node acts as both a source node sending its own data and a relay forwarding its partner's data to the destination. Mutual cooperation between neighboring nodes is believed to improve the overall system error performance, especially when space-time codes are incorporated. However, a comprehensive performance analysis of space-time-coded fully cooperative communication from all three perspectives, namel,y error performance, outage probability, and energy efficiency, is still missing. Answers to the commonly asked questions of whether, in what conditions, and to what extent the space-time-coded fully cooperative communication is better than direct transmission are still unknown. Motivated by this fact and inspired by the increasing popularity of healthcare applications in wireless body area networks (WBANs), this paper derives for the first time a comprehensive performance analysis of a decode-and-forward space-time coded fully cooperative communication network in Rayleigh and Rician fading channels in either identically or non-identically distributed fading scenario. Numerical analysis of error performance, outage probability, and energy efficiency, validated by simulations, show that fully cooperative communication is better than direct transmission from all three aspects in many cases, especially at a low-power and low signal-to-noise ratio regime, which is a typical working condition in WBANs.

INDEX TERMS Cooperative communication, decode-and-forward, MIMO, space-time codes, outage probability, energy efficiency, wireless body area networks, symbol error rates, Rayleigh, Rician.

I. INTRODUCTION

A. BACKGROUND

Cooperative communication comprises two main streams, namely relay-based cooperative communication (widely known as cooperative communication in the literature) and fully cooperative communication (term adopted from [1]) which is substantially different from its counterpart (as detailed below). To distinguish between the relay-based cooperative (i.e., the well-known cooperative communication) networks and the fully cooperative communication networks, in this paper, we refer the former to as *relay networks* and the latter to as *fully cooperative networks*.

In relay networks, transmission from the sources to the destination is assisted by either a single or multiple relaying nodes, which do not transmit their own signals. To forward the signals from the sources to the destinations, relays typically use either an Amplify-and-Forward (AF) or a Decode-and-Forward (DF) technique [1], [2], although other less common techniques, such as coded cooperation [3], can also be used. The conventional AF and DF ideas have been extended to associate with Space-Time Block Codes (STBCs) to take advantage of Multiple-Input Multiple-Output (MIMO) systems to improve further the system performance. These combined systems are usually referred in the literature to as *(distributed) space-time coded cooperative communication*. Readers may refer to [4] and [5] for the background on MIMO and STBCs. The combination of AF (or DF) and STBC has been widely examined for the relay networks, such as in [6], [7], [8], and [9]. Various system performance analyses of AF and DF relay networks

associated with STBCs have also been reported recently. For instance, Tourki *et al.* [10] and Shi and Karasawa [11] derived the exact error performance of dual hop DF opportunistic relay networks where the best among the available relays is selected to forward the signal. Ho-Van [12] derived the outage analysis of cooperative underlay cognitive networks under the imperfect channel estimation condition. Akin *et al.* [13] derived the error performance analysis of a DF relay network with relay selection in Nakagami-m channels, while Karademir and Altunbas [14] analyzed the error performance of a single AF relay network under the generalized-K channels. Wang and Hao [15] derived the closed-form expressions of the symbol error rate as well as the outage probability of a multiple relay network in Rayleigh fading channels. More recent works proposed relay selection strategies for MIMO AF two-way relay networks [16], a new cognitive radio system for primary users based on a two-path AF relaying scheme employing two secondary users [17], and quadrature spatial modulations in AF relaying systems [18], [19]. Recent works also focus on the energy harvesting perspectives in relay networks. For example, [20] jointly optimized the base station transmit power and the relay transmit power in a multicell AF relay network. [21] proposed the deployment of extra energy harvesting nodes as relays in an existing non-energy harvesting network, while [22] investigated the performance of energy harvesting protocols, namely time switching relaying and power splitting relaying, in two-hop cooperative relaying systems. Again, it is worth noting that, regardless of their particular name, most of the existing works in the literature only considered relay networks, rather than fully cooperative networks. *Relay networks have been intensively researched and thus are out of the scope of this paper.*

Unlike relay networks (i.e., the well-known cooperative networks), a fully cooperative network [1] refers to the network where nodes act as both source nodes transmitting their own data, and as relays retransmitting the signals for their partners. Additionally, fully cooperative communication can be applied to a multi-user network where each user (source node or sensor) collects, for example, different types of human bodies' physiological parameters, and multiple users (source nodes) cooperate with each others to transmit their data to the destination (a hub). For this reason, fully cooperative networks are also referred to as user cooperative networks in this particular context. Finally, because nodes are not only able to send their data but also capable of forwarding data for their partners, by their nature, fully cooperative networks facilitate a mesh topology between sensors and coordinators, which have been recently researched, such as by European Commission and European Union [23, p.9192], [24], [25].

In fully cooperative networks, source and destination nodes are within the coverage of each others. Possible applications of fully cooperative communication systems include emerging Wireless Body Area Networks (WBAN), Body Area Nano Networks (BANNs) [26], Wireless Sensor Networks (WSNs), Internet of Things (IoT) and indoor entertainment applications. While relay networks have been extensively researched, fully cooperative networks have been far less researched because these networks are more application-targeted. Answers for commonly asked questions, such as in what conditions and to what extent a fully cooperative network is better than a direct transmission system from all three perspectives, namely error performance, outage probability, and energy efficiency, are still missing in the literature. To the best of our knowledge, the closest work to this topic is [27] where the authors devised the symbol error rate (i.e., the error performance perspective) of a fully cooperative system with single-antenna nodes and BPSK modulation in identically distributed flat Rayleigh fading channels. However, neither an exact error rate analysis of a fully cooperative system in both identically and non-identically distributed Rayleigh and Rician fading channels with arbitrary M-PSK modulation and multi-antenna nodes, nor a comprehensive energy efficiency analysis of such systems is available. Given that very high speed, low error rate, highly energy efficient communications techniques are desperately desired in nowadays WBANs, IoT, and entertainment applications, especially at a low signal-to-noise regime, such in-depth analyses are extremely important to decide whether and when fully cooperative communication should be used, instead of direct transmission. Addressing these matters is the main motivation and contribution of this paper.

On the other hand, WBANs have been considerably researched recently to satisfy the ever-increasing needs of reliable, high speed, power efficient remote healthcare services. While WBANs are a daughter-class of more generic WSNs, the former have some important specifications that are distinct from the latter. WBANs are networks of sensors monitoring physiological parameters of human bodies. WBANs may include implantable and wearable sensors placed in, on, or near human bodies, thus wireless channels are classified into implant-to-implant, implant-to-on-body, implant-to-external, on-body to on-body and on-body to external channels. To assort many measurement campaigns, IEEE Technical Group 6 within the IEEE 802.15 committee has standardized the WBAN channel models in Nov. 2010 [29]. Frequency bands are 402–405 MHz for implant communication, and 5–50, 400, 600, 900, 2400 MHz (narrow bands) and 3.1–10.6 GHz (ultra-wideband - UWB) for on-body communication. Due to the movement of human bodies and the different characteristics of layers of body tissues as well as of the skin itself, propagation models for WBANs are distinct in various different scenarios as detailed in [29], compared to generic WSNs. Considering a narrowband WBAN at 900 MHz for instance, while the channel impulse responses can be modeled by a Rician distribution (or Rayleigh one if there is no line-of-sight link) for both on-body to on-body and on-body to external links, pathloss of on-body to on-body links follows the model named IEEE WBAN CM3 pathloss model and pathloss of the on-body to external links follows the CM4 pathloss model [29]. Note that, [30] claimed that a small-scale

fading model based on a gamma distribution is far better than the IEEE WBAN CM3 model. Due to the lack of available closed forms of many complicated expressions involved in a gamma distribution and due to our primary purpose to examine the comparative performance of the cooperative network in comparison with the direct transmission and the conventional Alamouti transmission, we follow the Rayleigh and Rician models for narrowband WBANs for simplicity.

Other important requirements of WBANs are their strict power constraint, battery lifetime and maximum radiation power due to health and safety reasons. For example, for MICS (Medical Implant Communication Service), the maximum power limitation is set to 25 μW (-16.02 dBm) EIRP (Equivalent Isotropically Radiated Power) by the FCC (Federal Communications Commission) [31, p.3], and 25 μW ERP (Effective Radiated Power) (i.e., 15.24 μW or -17.17 dBm EIRP) by the ETSI (European Telecommunications Standards Institute) [32, p.21]. In addition, the FCC limit for radio frequency (RF) exposure should not exceed the Specific Absorption Rate (SAR) of 1.6 W/kg for wireless devices, averaged over one gram of tissues, and 80 mW/kg for the whole body exposure [33, p.19]. Further, for UWB bands, peak transmission power is limited at -41.3 dBm/MHz (-14.31 dBm for a bandwidth of 500 MHz). As a result, WBANs work typically at a low power, low signal-to-noise regime.

B. RELATED WORKS

Fully cooperative networks potentially provide an improvement in the system error performance, data rate, coverage range, battery lifetime or a combination of those factors of WBANs. One of the common concerns about cooperative communication is whether cooperation is more power efficient than direct transmission, mainly due to the additional power consumption of the relays or neighbor nodes involving in the cooperation. This concern has been addressed positively in the literature (for relay networks only), such as [34] where the authors examined the symbol error rate and energy efficiency of a non-STBC relay network in WSNs, and in [35], where the authors examined a dynamic transmission scheme for a temporally and spatially correlated relay network in WBANs. However, to the best of our knowledge, an in-depth analysis of a decode-and-forward, space-time coded, fully cooperative communication network from all three perspectives, namely error performance, outage probability and energy efficiency, has been almost unexplored in the literature. To the best of our knowledge, the closest works to our paper are [27] and [28]. Tran *et al.* [27] devised the symbol error rate (SER) of a fully cooperative single carrier system, with single-antenna nodes and BPSK modulation, in identically distributed flat Rayleigh fading channels. However, [27] did not consider a fully cooperative system in non-identically distributed Rayleigh channels. It did not consider an arbitrary M-PSK modulation and multi-antenna nodes. Tran and Mertins [28] overcame some of the above shortages and considered a multi-carrier (OFDM) system. However, neither Rician fading channels nor outage probability analysis were mentioned there. Addressing these matters is the main motivation and contribution of this paper.

This paper devises a comprehensive performance analysis of the decode-and-forward, space-time block coded, fully cooperative communication network in both identically and non-identically distributed Rayleigh and Rician flat fading channels (these channels are applicable to the narrow band WBANs at 5–50, 400, 600, 900, and 2400 MHz) from all three perspectives, namely error performance, outage probability and energy efficiency. It is worth noting that, though WBANs are our primary inspiration, the analysis in this paper is not only applicable to WBANs, but also applicable to generic Rayleigh and Rician wireless environments.

C. CONTRIBUTIONS

The novel contributions of this paper include

1) For the first time, exact symbol error rate (SER) of the decode-and-forward, space-time block coded, fully cooperative communication network has been derived in both cases, namely identically distributed fading and non-identically distributed fading (detailed in the next section), with an arbitrary number of receive antennas at each node and an arbitrary M-PSK modulation scheme. Extension of these SER formulas to an arbitrary M-QAM modulation scheme is straightforward but tedious. Thus guidelines for this extension have been provided, but details will not be mentioned in the paper. The validity of the SER formulas has been confirmed by simulations. The error performance analysis shows that the fully cooperative communication could be significantly better than direct transmission in many cases, especially at a low SNR regime, such as WBANs.
2) Lower bounds and a closed-form of the SER of fully cooperative systems have been derived and verified by simulations. In addition, a performance metric (i.e., the mathematical relationship between the internode SNRs and the uplink SNRs) for fully cooperative systems to be better than direct transmission has been derived.
3) Given certain channel knowledge, the formulated SER allows the source nodes to pre-justify whether their collaboration will be helpful, compared to their direct transmission, and thus to decide beforehand whether they should really engage in the cooperative communication or a direct transmission should be used instead. The pre-justifying ability is critical in keeping the network operation as simple as possible, improving the network energy efficiency, while ensuring cooperative communication always useful once it is in place. Note that a proposal of a switching algorithm back and forth between direct transmission and cooperative communication modes is out of the scope of this paper.
4) A closed form of the outage probability has been presented for arbitrary M-PSK modulation. Accuracy of the approximated outage probabilities is examined

TABLE 1. Notations and terms used throughout the paper.

Parameter/term	Meaning
S_1, S_2, D	two source nodes (or users in a multi-user network) and destination node
n_T, n_R	number of transmit (TX) and receive (RX) antennas per node
G_T (dB), G_R (dB)	gain of the TX antenna and the RX antenna
L_c (dB)	total loss of connectors at both TX and RX antennas
M	constellation size of unit-energy M-PSK modulation
$S_1 \leftrightarrow S_2$	internode links
$S_1 \leftrightarrow D$, $S_2 \leftrightarrow D$	uplinks
γ	instantaneous SNR per symbol
$\bar{\gamma}_{ij}$, $\bar{\gamma}_{u1}$, $\bar{\gamma}_{u2}$	average SNR per symbol per branch in the internode links and uplinks
$\bar{\gamma}_{th}$	threshold of the average SNR per symbol
d_{ij} and d_u	distance of the internode links and the uplinks (assume that $d_{u1} \approx d_{u2} := d_u$)
Lower/upper case bold letters	vectors and matrices, respectively
$(.)^*$, $(.)^{\mathrm{T}}$, $(.)^{\mathrm{H}}$	complex conjugation, transposition, Hermitian transposition
$P(\Xi)$	probability of the random event Ξ
$\mathcal{CN}(0, \sigma^2)$, $Rayleigh(\bar{\gamma})$	complex Gaussian and Rayleigh distributions with the corresponding parameters
$Exp(\lambda)$, $Double-Exp(\lambda)$	exponential distribution and double-exponential distribution with the parameter λ
$\mathcal{P}_{pa}$, $\mathcal{P}_{ct}$, $\mathcal{P}_{cr}$, $\mathcal{P}_{bb}$	average power consumed by the power amplifier, TX circuit, RX circuit, and baseband circuit
'cooperative system'	fully cooperative system (not the well-known cooperative communication)
'direct transmission'	transmission from one source (e.g., S_1) to D without cooperation
'conventional Alamouti transmission'	transmission of the Alamouti code in a non-distributed, non-cooperative system

against the simulations. The outage analysis indicates that cooperative communication not only potentially improves the system error performance, but it is also better than direct transmission from the outage perspective in many cases.

5) Energy efficiencies of the direct transmission and of the fully cooperative network have been formulated. Again, the accuracy of these formulas has been confirmed by simulations. The energy efficiency analysis confirms that cooperative communication is worthwhile to be used over direct transmission from the power perspective in many cases, especially in WBAN applications at low transmission power regimes.
6) Theoretical analyses and simulations show that the fully cooperative networks might be better than the direct transmission from all three perspectives, namely error performance, outage probability and energy efficiency in many cases, especially at a lower SNR and lower power regime. This makes the fully cooperative networks really useful for emerging low-power applications, including WBANs.

The rest of this paper is constructed as follows. Section II presents the system model. Section III analyzes SER of the cooperative communications system in Rayleigh and Rician fading channels with both identically and non-identically distributed branch scenarios. Section IV analyzes the outage probability of the cooperative system. Energy efficiencies of both direct transmission system and cooperative system are analyzed in Section V. Section VII presents numerous numerical and simulated results from all three aspects, namely, symbol error rates, outage probabilities and energy efficiencies of the cooperative system, in comparison with the direct transmission and the conventional Alamouti transmission. Finally, Section VIII concludes the paper.

Notations: Throughout the paper, we use the notations and terms listed in Table 1.

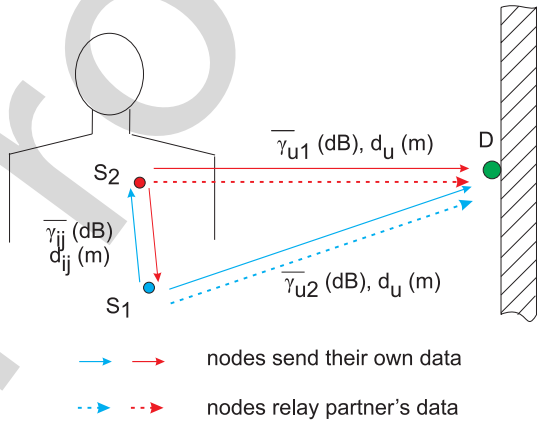

FIGURE 1. Network topology of the fully cooperative communication system.

II. SYSTEM MODEL

Network topology considered in this paper is depicted in Fig. 1. While this figure depicts a typical wireless body area network configuration, it is worth noting that this research could also be applied to other applications, such as home entertainment, Internet of Things (IoT), and generic sensor networks. Each node is equipped with one TX antenna and n_R RX antennas ($n_R = 1$ is a typical scenario). Average SNR per symbol per branch of the internode links is denoted as $\bar{\gamma}_{ij}$ and that of the uplinks from the source S_1 (S_2) to the destination as $\bar{\gamma}_{u1}$ ($\bar{\gamma}_{u2}$). Adopting the words from [36], we refer the case $\bar{\gamma}_{u1} = \bar{\gamma}_{u2} = \bar{\gamma}_u$ to as the identically distributed branches, and as the non-identically distributed branches if otherwise. Generally, $\bar{\gamma}_{ij}$ is different from $\bar{\gamma}_{u1}$ and $\bar{\gamma}_{u2}$. We assume that the distance from S_1 and D is approximately the same as that from S_2 to D, i.e., $d_{u1} = d_{u2} = d_u$. Channels between nodes experience block flat fading, i.e., channel coefficients h_{12} and h_{21} between the source nodes as well as h_1 and h_2 between the sources and the destination are constant during the transmission of an Alamouti Space-Time Block Code (STBC) [4], but change randomly from blocks to blocks. Channel coefficients

are independent, identically or non-identically distributed complex random variables following either the Rayleigh distribution *Rayleigh*(1) or a Rician distribution, while noises are independently identically distributed complex random variables following the Gaussian distribution $\mathcal{CN}(0, \sigma^2)$. The ratio between the average symbol power and noise power $\bar{\gamma} = E_S/\sigma^2$ is the average SNR per symbol per branch. Nodes are assumed to transmit uncoded M-PSK signals in either a half duplex mode or a full duplex mode (the transmission mode will be clarified clearly in each context), and to receive signals using Maximum Ratio Combining (MRC) techniques. Source nodes forward their partner data to the destination using the decode-and-forward (DF) technique in a distributed Alamouti STBC fashion. Three possible half- and full duplex transmission modes in the decode-and-forward space-time block coded fully cooperative communication system are detailed in Table 2.

TABLE 2. Possible transmission schemes in a decode-and-forward space-time block coded fully cooperative communication network.

(a) Half duplex (TDMA-based cooperative communication)

Time slot 1	Time slot 2	Time slot 3	Time slot 4
$\frac{s_1}{\sqrt{2}}\ (S_1 \to S_2, D)$	$\frac{s_2}{\sqrt{2}}\ (S_2 \to S_1, D)$	$-\frac{\acute{s}_2^*}{\sqrt{2}}\ (S_1 \to D)$	$\frac{\acute{s}_1^*}{\sqrt{2}}\ (S_2 \to D)$

(b) Half duplex

Time slot 1	Time slot 2	Time slot 3
$\frac{s_1}{\sqrt{2}}\ (S_1 \to S_2, D)$	$\frac{s_2}{\sqrt{2}}\ (S_2 \to S_1, D)$	$-\frac{\acute{s}_2^*}{\sqrt{2}}\ (S_1 \to D)$ $\frac{\acute{s}_1^*}{\sqrt{2}}\ (S_2 \to D)$

(c) Full duplex

Time slot 1	Time slot 2
$\frac{s_1}{\sqrt{2}}\ (S_1 \to S_2, D)$	$-\frac{\acute{s}_2^*}{\sqrt{2}}\ (S_1 \to D)$
$\frac{s_2}{\sqrt{2}}\ (S_2 \to S_1, D)$	$\frac{\acute{s}_1^*}{\sqrt{2}}\ (S_2 \to D)$

The first scheme is the conventional Time Division Multiple Access (TDMA)-based half-duplex mode where each source node transmits signals in one time slot. The complete transmission round requires four time slots. $\acute{s}$ denotes the forwarded version of the corresponding partner's signal s, which might possibly be different from s due to the transmission errors in the internode links. The second scheme is basically similar to the first, except that the sources forward the partner's signals in the same time slot, thus the transmission round requires three time slots to complete. The last scheme is a full duplex mode where the source nodes can transmit and receive signals in the same time slots. The full duplex mode is possible, for example, when nodes transmit and receive signals on different frequency bands. Multiband Orthogonal Frequency Division Multiplexing Ultra-Wideband (MB-OFDM UWB) systems standardized in [37] are an example technique where full duplex cooperative communication is feasible as shown in a number of publications [38], [39]. We can realize that, there are two main phases in all three schemes, namely the internode information exchange (Phase I), where the source nodes exchange their own data with their partner, and the (distributed) Alamouti space-time block coded transmission (Phase II), where an Alamouti-like space-time code $\frac{1}{\sqrt{2}}[s_1 \quad s_2; \quad -\acute{s}_2^* \quad \acute{s}_1^*]$ is effectively transmitted from the sources to the destination. Specifically, for all three schemes in Table 2, Phase I involves in all time slots except the last time slot, while Phase II involves in all time slots, including the last one.

The signal s_i transmitted from S_i, $i \in \{1, 2\}$, will be estimated by the partner S_j, $j \in \{1, 2 | j \neq i\}$ as $\acute{s}_i$ based on the following MRC decision metric after Phase I completes

$$\acute{s}_i \leftarrow \hat{s}_i = r_{ij} h_{ij}^{\mathrm{H}}, \tag{1}$$

where $r_{ij} = \frac{1}{\sqrt{2}} h_{ij} s_i + n_{ij}$ is the received signal at S_j, $h_{ij} = [h_{ij,1}, \ldots, h_{ij,n_R}]$ is the channel vector between S_i and S_j, and $n_{ij} = [n_{ij,1}, \ldots, n_{ij,n_R}]$ is the noise vector at n_R RX antennas of S_j. Note that $\acute{s}_i$ might be different from s_i due to transmission errors in the internode links. After detecting s_i, the source nodes will forward the estimated signals to the destination in the next time slots in the forms of $-\acute{s}_2^*$ and $\acute{s}_1^*$ as shown in Table 2.

After Phase I and Phase II are completed, the received signals at the destination, respectively, are

$$\begin{aligned} r_1 &= \frac{1}{\sqrt{2}} h_1 s_1 + \frac{1}{\sqrt{2}} h_2 s_2 + n_1, \\ r_2 &= -\frac{1}{\sqrt{2}} h_1 \acute{s}_2^* + \frac{1}{\sqrt{2}} h_2 \acute{s}_1^* + n_2. \end{aligned} \tag{2}$$

Therefore, the transmitted signals s_1 and s_2 will be estimated based on the following MRC decision metrics

$$\begin{aligned} \underline{s}_1 &\leftarrow \tilde{s}_1 = r_1 h_1^{\mathrm{H}} + r_2^* h_2^{\mathrm{T}}, \\ \underline{s}_2 &\leftarrow \tilde{s}_2 = r_1 h_2^{\mathrm{H}} - r_2^* h_1^{\mathrm{T}}. \end{aligned} \tag{3}$$

Note that s_i, $\acute{s}_i$ and $\underline{s}_i$ are all M-PSK symbols, and that the factor $\frac{1}{\sqrt{2}}$ in Table 2 as well as in the above formulas is to guarantee the total average transmission power from the two source nodes to the destination during the Alamouti transmission process is always one, which is the same as that in a single antenna, direct transmission system for a fair comparison.

III. SYMBOL ERROR RATE

The analysis in this section can be applied to any of the three schemes in Table 2. Denote P_{ij} and P_A as the Symbol Error Rate (SER) of the internode link $S_i - S_j$ and of the Alamouti STBC transmission, respectively, assuming that M-PSK modulation is used in all links in the system. Denote Φ and Ψ as the events where the cooperative system has errors due to the erroneous information exchange between the sources and due to erroneous Alamouti transmission, respectively. Thus $\Phi + \Psi$ presents the event where the cooperative system has errors. Since Φ and Ψ are not mutually exclusive of one another, all possibilities of Φ and Ψ, indicated by the two circles in Fig. 2 and denoted as $P(\Phi)$ and $P(\Psi)$ respectively, might partially overlap each other. From this figure, we have the following probability equality

$$P(\Phi + \Psi) = P(\Psi) + P\big(\Phi | \bar{\Psi}\big), \tag{4}$$

where $P\big(\Phi | \bar{\Psi}\big)$ is the probability of Φ conditioned on the negation of Ψ. Eq. (4) can be interpreted as follows: SER of

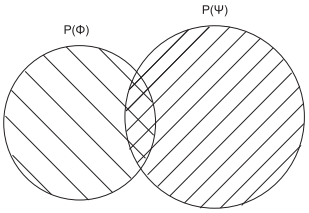

FIGURE 2. Component probability model for the symbol error rate analysis of the fully cooperative communication system.

the cooperative system equals the sum of SER of the Alamouti transmission (i.e., P_A) and SER of the cooperative system when there is no error during the Alamouti transmission. $P(\Phi|\bar{\Psi})$ can be written further as

$$P(\Phi|\bar{\Psi}) = P(\Phi|\bar{\Psi}, \not{s}_1) + P(\Phi|\bar{\Psi}, \not{s}_2) + P(\Phi|\bar{\Psi}, \not{s}_1, \not{s}_2), \quad (5)$$

where the three terms on the right side of Eq. (5) stand for SER of the cooperative communication system when s_1 is erroneous (s_2 is correct), s_2 is erroneous (s_1 is correct), and both are erroneous, respectively. Note that no error occurs in the uplinks.

Because two internode links $S_1 \rightarrow S_2$ and $S_2 \rightarrow S_1$ are independent fading channels with the same average SNR, $\bar{\gamma}_{ij}$, it is reasonable to assume the probabilities that the link $S_1 \rightarrow S_2$ is erroneous (while $S_2 \rightarrow S_1$ is good), that $S_2 \rightarrow S_1$ is erroneous ($S_1 \rightarrow S_2$ is good), that both are good, and that both are erroneous are all 0.25. Given that P_{ij} is the symbol error probability of a M-PSK transmission over a fading channel, the probability of either symbol being erroneous in that fading channel is $0.25P_{ij}(1-P_{ij})$, resulting in the SER of the cooperative system in this case being $P(\Phi|\bar{\Psi}, \not{s}_1) = P(\Phi|\bar{\Psi}, \not{s}_2) = 0.25P_{ij}(1-P_{ij})(1-P_A)$. Similarly, the probability that both transmissions are erroneous in the considered fading channel is $0.25P_{ij}^2$, resulting in the SER of the cooperative communication system in this case being $P(\Phi|\bar{\Psi}, \not{s}_1, \not{s}_2) = 2 \times 0.25P_{ij}^2(1-P_A) = 0.5P_{ij}^2(1-P_A)$, where the factor 2 reflects that there are two symbol errors. As a result, Eq. (5) becomes

$$\begin{aligned} P(\Phi|\bar{\Psi}) &= 0.5P_{ij}(1-P_{ij})(1-P_A) + 0.5P_{ij}^2(1-P_A) \\ &= 0.5(1-P_A)P_{ij}. \end{aligned} \quad (6)$$

From Eqs. (4) and (6), SER of the cooperative communication system is

$$P_C := P(\Phi + \Psi) = P_A + 0.5(1-P_A)P_{ij}. \quad (7)$$

We now work out the formulas of SER of the information interchange process, P_{ij}, and the Alamouti transmission process, P_A, in two scenarios, namely identically distributed branches and non-identically distributed branches, in both Rayleigh and Rician fading scenarios.

A. RAYLEIGH FADING CHANNELS

1) IDENTICALLY DISTRIBUTED BRANCHES

In this case, average SNRs of the uplinks from all source nodes to the destinations are all the same, i.e., $\bar{\gamma}_{u1} = \bar{\gamma}_{u2} = \bar{\gamma}_u$. It is known that SER of a M-PSK modulation in a MRC system with one TX antenna and n_R RX antennas in Rayleigh fading channels is [36, Eq.(9.15)]

$$P_{MRC} = \frac{1}{\pi}\int_0^{(M-1)\pi/M} \left(1 + \frac{\bar{\gamma}\sin^2(\pi/M)}{\sin^2(\phi)}\right)^{-n_R} d\phi, \quad (8)$$

where $\bar{\gamma}$ denotes the average SNR per symbol per channel branch.

From Eq. (8), we can derive the SER formula of the internode links as

$$P_{ij} = \frac{1}{\pi}\int_0^{(M-1)\pi/M} \left(1 + \frac{\bar{\gamma}_{ij}\sin^2(\pi/M)}{\sin^2(\phi)}\right)^{-n_R} d\phi, \quad (9)$$

where $\bar{\gamma}_{ij}$ denotes the average SNR per symbol per channel branch of the internode links. Meanwhile, SER of the direct transmission link from S_1 (same for S_2) to the destination, P_D, is

$$P_D = \frac{1}{\pi}\int_0^{(M-1)\pi/M} \left(1 + \frac{\bar{\gamma}_u\sin^2(\pi/M)}{\sin^2(\phi)}\right)^{-n_R} d\phi. \quad (10)$$

Error performance of the conventional Alamouti STBC in a $2In_RO$ (2 TX antennas, n_R RX antennas) configuration is 3dB worse than that of the corresponding MRC system with $2n_R$ RX antennas due to the fact that power per symbol transmitted from each TX antenna in the Alamouti process is half that power in the MRC system [4]. Therefore, SER of the Alamouti STBC, P_A, in the a $2In_RO$ configuration in Rayleigh fading channels can be found by replacing $\bar{\gamma}$ by $\bar{\gamma}_u/2$ in the SER formula of the $1I2n_RO$ MRC system, i.e.,

$$P_A = \frac{1}{\pi}\int_0^{(M-1)\pi/M} \left(1 + \frac{\bar{\gamma}_u\sin^2(\pi/M)}{2\sin^2(\phi)}\right)^{-2n_R} d\phi, \quad (11)$$

where $\bar{\gamma}_u$ denotes the average SNR per symbol per channel branch of the uplinks.

From Eqs. (7), (9) and (11), SER of the cooperative communication system is given in Eq. (12).

$$\begin{aligned} P_C = &\frac{1}{\pi}\int_0^{(M-1)\pi/M} \left(1 + \frac{\bar{\gamma}_u\sin^2(\pi/M)}{2\sin^2(\phi)}\right)^{-2n_R} d\phi \\ &+\left[1 - \frac{1}{\pi}\int_0^{(M-1)\pi/M} \left(1 + \frac{\bar{\gamma}_u\sin^2(\pi/M)}{2\sin^2(\phi)}\right)^{-2n_R} d\phi\right] \\ &\times \frac{1}{2\pi}\int_0^{(M-1)\pi/M} \left(1 + \frac{\bar{\gamma}_{ij}\sin^2(\pi/M)}{\sin^2(\phi)}\right)^{-n_R} d\phi. \end{aligned} \quad (12)$$

2) NON-IDENTICALLY DISTRIBUTED BRANCHES

In this case, average SNRs of the uplinks from the source nodes to the destinations are not the same, i.e., $\bar{\gamma}_{u1} \neq \bar{\gamma}_{u2}$. It is reasonable to assume that the average SNRs of the links from the i-th ($i = \{1, 2\}$) source node to n_R RX antennas of the destination are the same and equal to $\bar{\gamma}_{ui}$. Similarly, the average SNRs of the links between a source node to n_R RX antennas of its partner are also assumed to be the same and are equal to $\bar{\gamma}_{ij}$. A typical example for the non-identically distributed scenario is when the doctor's or patient's identity card or a badge impedes persistently the uplinks from one source node to the destination, while they do not obstruct the

other source node. M-PSK modulation and Rayleigh fading channels are still being considered here. SER of the direct transmission link from S_1 (S_2) to the destination, denoted as $P_{D1(2)}$, can be found as below [36, eq.(9.15)]

$$P_{D1(2)} = \frac{1}{\pi}\int_0^{(M-1)\pi/M}\left(1+\frac{\bar{\gamma}_{u1(2)}\sin^2(\pi/M)}{\sin^2(\phi)}\right)^{-n_R}d\phi. \tag{13}$$

SER of the Alamouti STBC, P_A, in this scenario would be

$$P_A = \frac{1}{\pi}\int_0^{(M-1)\pi/M}\left(1+\frac{\bar{\gamma}_{u1}\sin^2(\pi/M)}{2\sin^2(\phi)}\right)^{-n_R} \times\left(1+\frac{\bar{\gamma}_{u2}\sin^2(\pi/M)}{2\sin^2(\phi)}\right)^{-n_R}d\phi, \tag{14}$$

It is worth noting that, Eqs. (11) and (14) are the exact SERs of the conventional Alamouti STBC with an arbitrary M-PSK modulation scheme in the identically distributed branches and non-identically distributed branches, respectively. Compared to the SER formulas devised in the literature, such as in [40, eq.(46)], [41], [42, eq.(12)], these formulas are much more concise and easier to be calculated by Matlab. Derivation of these two equations, especially, Eq. (14) for non-identically distributed branches, is also a novel contribution of our paper. SER of the internode links, P_{ij}, still follows Eq. (9). From Eqs. (7), (9) and (14), SER of the cooperative communication system is given in Eq. (15).

$$\begin{aligned}P_C = {}& \frac{1}{\pi}\int_0^{(M-1)\pi/M}\left(1+\frac{\bar{\gamma}_{u1}\sin^2(\pi/M)}{2\sin^2(\phi)}\right)^{-n_R} \times\left(1+\frac{\bar{\gamma}_{u2}\sin^2(\pi/M)}{2\sin^2(\phi)}\right)^{-n_R}d\phi \\ &+\left[1-\frac{1}{\pi}\int_0^{(M-1)\pi/M}\left(1+\frac{\bar{\gamma}_{u1}\sin^2(\pi/M)}{2\sin^2(\phi)}\right)^{-n_R} \times\left(1+\frac{\bar{\gamma}_{u2}\sin^2(\pi/M)}{2\sin^2(\phi)}\right)^{-n_R}d\phi\right] \\ &\times\frac{1}{2\pi}\int_0^{(M-1)\pi/M}\left(1+\frac{\bar{\gamma}_{ij}\sin^2(\pi/M)}{\sin^2(\phi)}\right)^{-n_R}d\phi.\end{aligned} \tag{15}$$

By modifying [36, eq. (9.26)] in a similar procedure applied to Eqs. (8-15), we can easily derive SERs of the cooperative communication for M-QAM modulation schemes in both identically distributed and non-identically distributed cases. The extension of Eqs. (12) and (15) to an arbitrary M-QAM modulation scheme is straightforward. Due to the limited space, this extension will not be explained here, but in another publication.

B. RICIAN FADING CHANNELS

Let us consider the cooperative system with one TX antenna and n_R RX antennas at each node, using M-PSK modulation. Similarly to Section III-A.2, in the non-identically distributed scenario, it is reasonable to assume that the average SNR per symbol per branch from S_1 (S_2 respectively) to each of the n_R RX antennas of the destination is the same, denoted as $\bar{\gamma}_{u1}$ ($\bar{\gamma}_{u2}$), but the average SNR per symbol per branch from different source nodes to the RX antennas of the destination are not the same, i.e., $\bar{\gamma}_{u1} \neq \bar{\gamma}_{u2}$. Each branch from S_1 (S_2) to n_R RX antennas of the destination is a Rician fading channel with a K-factor, denoted as K_1 (K_2). Further, denote $\kappa_n = \sqrt{K_n}$ and the Moment Generating Function (MGF) of the SER of the n-th branch ($n \in \{1,\ldots,n_R\}$) of this MRC system as $M_{\bar{\gamma}_n}(s)$. Then the MGF will be calculated as [36, Table 9.1]

$$M_{\bar{\gamma}_n}(s) = \frac{1+\kappa_n^2}{1+\kappa_n^2-s\bar{\gamma}_n}\exp\left(\frac{\kappa_n^2 s\bar{\gamma}_n}{1+\kappa_n^2-s\bar{\gamma}_n}\right). \tag{16}$$

SER of this MRC system will be [36, eq.(9.15)]

$$P_{MRC} = \frac{1}{\pi}\int_0^{(M-1)\pi/M}\prod_{n=1}^{n_R}M_{\bar{\gamma}_n}\left(-\frac{\sin^2(\pi/M)}{\sin^2(\phi)}\right)d\phi. \tag{17}$$

Therefore, SER of the internode links is computed as

$$P_{ij} = \frac{1}{\pi}\int_0^{(M-1)\pi/M}\left[M_{\bar{\gamma}_{ij}}\left(-\frac{\sin^2(\pi/M)}{\sin^2(\phi)}\right)\right]^{n_R}d\phi, \tag{18}$$

and SER of the direct transmission from S_1 (S_2) to the destination is

$$P_{D1(2)} = \frac{1}{\pi}\int_0^{(M-1)\pi/M}\left[M_{\bar{\gamma}_{u1(2)}}\left(-\frac{\sin^2(\pi/M)}{\sin^2(\phi)}\right)\right]^{n_R}d\phi. \tag{19}$$

By modifying Eq. (17) and noting that the average SNR per branch among n_R branches from S_1 (or S_2) to D being $\bar{\gamma}_{u1}/2$ ($\bar{\gamma}_{u2}/2$ respectively), the Alamouti transmission in non-identically distributed Rician fading channels would be

$$P_A = \frac{1}{\pi}\int_0^{(M-1)\pi/M}\left[M_{0.5\bar{\gamma}_{u1}}\left(-\frac{\sin^2(\pi/M)}{\sin^2(\phi)}\right)\right]^{n_R} \times\left[M_{0.5\bar{\gamma}_{u2}}\left(-\frac{\sin^2(\pi/M)}{\sin^2(\phi)}\right)\right]^{n_R}d\phi. \tag{20}$$

From Eqs. (7), (18) and (20), SER of the cooperative communication with an arbitrary M-PSK modulation scheme in Rician fading channels in the non-identically distributed scenario can be written as

$$\begin{aligned}P_C = {}& \frac{1}{\pi}\int_0^{(M-1)\pi/M}\left[M_{0.5\bar{\gamma}_{u1}}\left(-\frac{\sin^2(\pi/M)}{\sin^2(\phi)}\right)\right]^{n_R} \times\left[M_{0.5\bar{\gamma}_{u2}}\left(-\frac{\sin^2(\pi/M)}{\sin^2(\phi)}\right)\right]^{n_R}d\phi \\ &+\left[1-\frac{1}{\pi}\int_0^{(M-1)\pi/M}\left[M_{0.5\bar{\gamma}_{u1}}\left(-\frac{\sin^2(\pi/M)}{\sin^2(\phi)}\right)\right]^{n_R} \times\left[M_{0.5\bar{\gamma}_{u2}}\left(-\frac{\sin^2(\pi/M)}{\sin^2(\phi)}\right)\right]^{n_R}d\phi\right] \\ &\times\frac{1}{\pi}\int_0^{(M-1)\pi/M}\left[M_{\bar{\gamma}_{ij}}\left(-\frac{\sin^2(\pi/M)}{\sin^2(\phi)}\right)\right]^{n_R}d\phi.\end{aligned} \tag{21}$$

Derivation of the exact SER expressions of the Alamouti STBC system and the cooperative communication system (cf. Eqs. (20) and (21)) with M-PSK modulation schemes in Rician fading channels in both identically and non-identically distributed branches is another novel contribution of our paper.

A special case of the non-identically distributed case is the identically distributed case where $\bar{\gamma}_{u1} = \bar{\gamma}_{u2} = \bar{\gamma}_u$. By replacing $\bar{\gamma}_{u1}$ and $\bar{\gamma}_{u2}$ by $\bar{\gamma}_u$ in Eqs. (19) and (20), we can easily derive the SER formulas of the direct transmission and the cooperative communication systems in the identically distributed branches.

We have derived the SER expressions of the direct transmission system, the conventional (non-cooperative) Alamouti system, and the cooperative communication system in very general cases, which will be plotted against each other later in Section VII for comparing and evaluating the usefulness of the cooperative communication system. It is worth noting that, for the Gray mapping, the conventional lower bound of the Bit Error Rate (BER) of the M-PSK or M-QAM cooperative system, P_{bC}, can be calculated from SER as $P_{bC} = P_C/\log_2(M)$ [43]. More accurate estimations of the BER lower bound in some specific modulation schemes can be found in the literature, such as [43, eq.(8)] for an 8-PSK modulation scheme.

IV. OUTAGE PROBABILITY

Beside SER, another important parameter to evaluate the performance of a MIMO system is outage probability. Outage probability of a MRC system is defined as the average probability that the instantaneous post-processing SNR, denoted as γ, at the output of the maximum ratio combiner does not exceed a certain SNR threshold, defined as $\bar{\gamma}_{th}$, i.e., $P_o = P(\gamma \le \bar{\gamma}_{th})$. Let us consider a Single-Input Single-Output (SISO) system in a Rayleigh channel, whose channel coefficient is denoted as h where $|h| \sim Rayleigh(1)$. The instantaneous SNR at the output of an identically distributed MRC receiver is $\gamma = \frac{E_S|h|^2}{\sigma^2} = \bar{\gamma}|h|^2$. It is known that the outage probability of this SISO system is [36, Table 9.5]

$$P_o^{\text{SISO}} = P(\bar{\gamma}|h|^2 \le \bar{\gamma}_{th})) = 1 - e^{-\bar{\gamma}_{th}/\bar{\gamma}}. \quad (22)$$

For brevity, instead of considering the term $\sqrt{\bar{\gamma}}|h|$ where $|h| \sim Rayleigh(1)$, we will consider the term $|\underline{h}| \sim Rayleigh(\bar{\gamma})$. The instantaneous SNR at output of a MRC system with 1 TX antenna and n_R RX antennas (i.e., $1\text{In}_\text{R}\text{O}$ system) is $\bar{\gamma} = \frac{E_S\sum_{n=1}^{n_R}|h_n|^2}{\sigma^2} = \sum_{n=1}^{n_R}|\underline{h}|^2$. Eq. (22) can be generalized for the $1\text{In}_\text{R}\text{O}$ MRC system as below [44, eq.(32)], which is the equation generalized from the outage probability of a dual branch MRC system reported in [36, eq.(9.246)]

$$P_o^{1\text{In}_\text{R}\text{O}} = P\left(\sum_{n=1}^{n_R}|\underline{h}|^2 \le \bar{\gamma}_{th})\right) = 1 - e^{-\bar{\gamma}_{th}/\bar{\gamma}}\left[\sum_{n=0}^{n_R-1}\frac{1}{n!}\left(\frac{\bar{\gamma}_{th}}{\bar{\gamma}}\right)^n\right]. \quad (23)$$

Hence, outage probability of the direct transmission from S_1 (same as S_2) to the destination is

$$P_o^{\text{D}} = 1 - e^{-\bar{\gamma}_{th}/\bar{\gamma}_u}\left[\sum_{n=0}^{n_R-1}\frac{1}{n!}\left(\frac{\bar{\gamma}_{th}}{\bar{\gamma}_u}\right)^n\right], \quad (24)$$

where $\bar{\gamma}_u$ is the average SNR per symbol in the uplink from S_i to the destination.

We now derive the outage probability of the conventional Alamouti STBC code. After some simple mathematical manipulations, the instantaneous SNR at the output of the MRC receiver in the Alamouti STBC system in a $2\text{In}_R\text{O}$ configuration, γ_A, can be written as $\gamma_A = \frac{\sum_{n=1}^{n_R}|\underline{h}_{1n}|^2+|\underline{h}_{2n}|^2}{2}$, where $\underline{h}_{in}$ is the channel coefficient of the n-th branch from S_i ($i = \{1, 2\}$) to the destination multiplied with $\sqrt{\bar{\gamma}_u}$. The formula of γ_A is similar to the instantaneous SNR value in the $1\text{I}2n_R\text{O}$ MRC system, except that γ_A has the factor $1/2$ since each TX antenna transmits half the symbol power used in the direct transmission for a fair comparison. Therefore, similarly to SER, outage probability of the Alamouti code in a $2\text{In}_R\text{O}$ configuration can be found from that of the $1\text{I}2n_R\text{O}$ MRC system (cf. Eq. (23)) with half the average SNR per branch (i.e., $\bar{\gamma}_u/2$). Thus the outage probability of the Alamouti STBC is

$$P_o^A = P\left(\frac{\sum_{n=1}^{n_R}|\underline{h}_{1n}|^2 + |\underline{h}_{2n}|^2}{2} \le \bar{\gamma}_{th})\right) = 1 - e^{-2\bar{\gamma}_{th}/\bar{\gamma}_u}\left[\sum_{n=0}^{2n_R-1}\frac{1}{n!}\left(\frac{2\bar{\gamma}_{th}}{\bar{\gamma}_u}\right)^n\right]. \quad (25)$$

Next, we will derive the outage probabilities of the direct transmission and the cooperative systems with arbitrary M-PSK modulation. For simplicity, we limit our consideration to the case of $n_R = 1$ RX antenna, which is a typical scenario in WBANs due to the small physical size of nodes. However, generalization of our analysis mentioned below for an arbitrary n_R is relatively straightforward. We limit our consideration to the case of identically distributed branches only. Also, due to the lack of available closed forms of some random distributions, we can only derive a close estimation of the system outage probability.

Since the system has identically distributed branches, the average system outage can be derived by considering the decoding metric for either s_1 or s_2. Without loss of generality, we will consider the decoding metric of s_1. From Eq. (3), given that $n_R = 1$, the decoding metric of s_1 can be written as

$$\tilde{s}_1 = \frac{1}{\sqrt{2}}|h_1|^2 s_1 + \frac{1}{\sqrt{2}}|h_2|^2\acute{s}_1 + \frac{1}{\sqrt{2}}h_1^* h_2(s_2 - \acute{s}_2) + h_1^* n_1 + h_2 n_2^*. \quad (26)$$

In Eq. (26), $\acute{s}_1$ and $\acute{s}_2$ are the detected symbols of s_1 and s_2 at the node S_2 and S_1, respectively. Hence we will derive four components of the outage probability corresponding to the four possible cases, depending whether $\acute{s}_1 = s_1$ and $\acute{s}_2 = s_2$. It is important to note that, in a general M-PSK

modulation using a Gray mapping, if $\acute{s}_i \neq s_i$, then $|s_i - \acute{s}_i|$ is likely the distance between two neighbor points in the M-PSK constellation, i.e., $|s_i - \acute{s}_i|^2 = 2[1 - \cos(2\pi/M)]$, and that $\acute{s}_i$ should be considered as noise when formulating the instantaneous SNR of s_i.

A. $s_1 = \acute{s}_1, s_2 = \acute{s}_2$

From Eq. (26), we can write the instantaneous SNR of the decoding metric of s_1 as

$$\gamma_c = \frac{(|\underline{h}_1|^2 + |\underline{h}_2|^2)}{2}, \tag{27}$$

where $\underline{h}_i = \sqrt{\bar{\gamma}_u} h_i$. From Eqs. (25) and (27), we have

$$\begin{aligned} P(\gamma_c \leq \bar{\gamma}_{th}) &= P\left(\frac{|\underline{h}_1|^2 + |\underline{h}_2|^2}{2} \leq \bar{\gamma}_{th}\right) \\ &= 1 - \mathrm{e}^{-2\bar{\gamma}_{th}/\bar{\gamma}_u}\left(1 + \frac{2\bar{\gamma}_{th}}{\bar{\gamma}_u}\right). \end{aligned} \tag{28}$$

Because the event $(s_1 = \acute{s}_1, s_2 = \acute{s}_2)$ occurs with the probability $(1 - P_{ij})^2$, where P_{ij} is SER of the internode link (cf. Eq. (9)), the first component of the outage probability of the cooperative system, denoted as P_{o1}^C, is

$$P_{o1}^C = (1 - P_{ij})^2\left[1 - \mathrm{e}^{-2\bar{\gamma}_{th}/\bar{\gamma}_u}\left(1 + \frac{2\bar{\gamma}_{th}}{\bar{\gamma}_u}\right)\right]. \tag{29}$$

TABLE 3. Comparison of the first and second moments.

	$\lvert\underline{h}_1\rvert^2\lvert\underline{h}_2\rvert^2$	$\sqrt{\frac{3}{80}}(\lvert\underline{h}_1\rvert^2 + \lvert\underline{h}_2\rvert^2)$
$\mathrm{E}\{.\}$	$\bar{\gamma}_u^2$	$1.15\bar{\gamma}_u^2$
$\mathrm{var}\{.\}$	$6\bar{\gamma}_u^4$	$6\bar{\gamma}_u^4$

B. $s_1 = \acute{s}_1, s_2 \neq \acute{s}_2$

Since $|s_i - \acute{s}_i|^2 = 2[1 - \cos(2\pi/M)]$, the instantaneous SNR of the decoding metric of s_1 is

$$\gamma_c = \frac{\left(|\underline{h}_1|^2 + |\underline{h}_2|^2\right)^2}{2[1 - \cos(\frac{2\pi}{M})]|\underline{h}_1|^2|\underline{h}_2|^2 + 2|\underline{h}_1|^2 + 2|\underline{h}_2|^2}. \tag{30}$$

Since $|\underline{h}| \sim Rayleigh(\bar{\gamma}_u)$, $|\underline{h}|^2$ follows an exponential distribution $|\underline{h}|^2 \sim Exp(\lambda_u)$, where $\lambda_u = 1/\bar{\gamma}_u$. As a result, $Z := |\underline{h}_1|^2|\underline{h}_2|^2$ is a random variable (RV) following a product distribution (or K distribution) [45] with the Probability Distribution Function (PDF) $2\lambda_u^2 K_0(z)$, where K_0 is the modified Bessel function of the zero order of the second kind. Due to the lack of a closed form of K_0 in the range of small values of λ_u (i.e., in the low range of $\bar{\gamma}_{th}/\bar{\gamma}_u$), we will approximate Z by $\sqrt{\frac{3}{80}}(|\underline{h}_1|^2 + |\underline{h}_2|^2)$, which has the first and second moments roughly equal to those of Z as shown in Table 3. These moments can be calculated following [46, p.70]. Eq. (30) now becomes

$$\gamma_c \approx \frac{\left(|\underline{h}_1|^2 + |\underline{h}_2|^2\right)}{\sqrt{\frac{3}{20}}\left[1 - \cos(\frac{2\pi}{M})\right](|\underline{h}_1|^2 + |\underline{h}_2|^2) + 2}. \tag{31}$$

From Eq. (23), we have

$$\begin{aligned} &P(\gamma_c \leq \bar{\gamma}_{th}) \\ &\approx P\left(\left(|\underline{h}_1|^2 + |\underline{h}_2|^2\right)\left[1 - \sqrt{\frac{3}{20}}\left(1 - \cos(\frac{2\pi}{M})\right)\bar{\gamma}_{th}\right] \leq 2\bar{\gamma}_{th}\right) \\ &= \begin{cases} 1, & \bar{\gamma}_{th} \geq \frac{\sqrt{\frac{20}{3}}}{\left[1 - \cos(\frac{2\pi}{M})\right]}; \\ 1 - e^{-\frac{2\bar{\gamma}_{th}}{\left[1 - \sqrt{\frac{3}{20}}\left(1 - \cos(\frac{2\pi}{M})\right)\bar{\gamma}_{th}\right]\bar{\gamma}_u}} & \\ \times\left(1 + \frac{2\bar{\gamma}_{th}}{\left[1 - \sqrt{\frac{3}{20}}\left(1 - \cos(\frac{2\pi}{M})\right)\bar{\gamma}_{th}\right]\bar{\gamma}_u}\right), & \bar{\gamma}_{th} < \frac{\sqrt{\frac{20}{3}}}{\left[1 - \cos(\frac{2\pi}{M})\right]}. \end{cases} \end{aligned} \tag{32}$$

The first equality is due to $\left(|\underline{h}_1|^2 + |\underline{h}_2|^2\right)\left[1 - \sqrt{\frac{3}{20}}\left(1 - \cos(\frac{2\pi}{M})\right)\bar{\gamma}_{th}\right] \leq 2\bar{\gamma}_{th}$ if $\bar{\gamma}_{th} \geq \frac{\sqrt{\frac{20}{3}}}{\left[1 - \cos(\frac{2\pi}{M})\right]}$. Since the case $(s_1 = \acute{s}_1, s_2 \neq \acute{s}_2)$ occurs with the probability $P_{ij}(1 - P_{ij})$, the second component of the outage probability of the cooperative system, P_{o2}^C, is

$$P_{o2}^C \approx \begin{cases} P_{ij}(1 - P_{ij}), & \bar{\gamma}_{th} \geq \frac{\sqrt{\frac{20}{3}}}{\left[1 - \cos(\frac{2\pi}{M})\right]}; \\ P_{ij}(1 - P_{ij}) & \\ \left[1 - e^{-\frac{2\bar{\gamma}_{th}}{\left[1 - \sqrt{\frac{3}{20}}\left(1 - \cos(\frac{2\pi}{M})\right)\bar{\gamma}_{th}\right]\bar{\gamma}_u}}\right] & \\ \times\left(1 + \frac{2\bar{\gamma}_{th}}{\left[1 - \sqrt{\frac{3}{20}}\left(1 - \cos(\frac{2\pi}{M})\right)\bar{\gamma}_{th}\right]\bar{\gamma}_u}\right)\Bigg], & \bar{\gamma}_{th} < \frac{\sqrt{\frac{20}{3}}}{\left[1 - \cos(\frac{2\pi}{M})\right]}. \end{cases} \tag{33}$$

C. $s_1 \neq \acute{s}_1, s_2 = \acute{s}_2$

The instantaneous SNR is calculated as

$$\gamma_c = \frac{|\underline{h}_1|^4}{|\underline{h}_2|^4 + 2|\underline{h}_1|^2 + 2|\underline{h}_2|^2}. \tag{34}$$

We consider two cases as below.

- $0 < \bar{\gamma}_{th} \leq 1$: The inequality $\gamma_c \leq \bar{\gamma}_{th}$ is equivalent to

$$|\underline{h}_1|^4 - 2\bar{\gamma}_{th}|\underline{h}_1|^2 + \bar{\gamma}_{th}^2 \leq \bar{\gamma}_{th}|\underline{h}_2|^4 + 2\bar{\gamma}_{th}|\underline{h}_1|^2 + \bar{\gamma}_{th}^2. \tag{35}$$

If $\bar{\gamma}_{th} \leq 1$, one has $\bar{\gamma}_{th}|\underline{h}_2|^4 + 2\bar{\gamma}_{th}|\underline{h}_2|^2 + \bar{\gamma}_{th}^2 \leq |\underline{h}_2|^4 + 2\bar{\gamma}_{th}|\underline{h}_2|^2 + \bar{\gamma}_{th}^2$. As a result, $P(\gamma_c \leq \bar{\gamma}_{th})$ is upper bounded by the probability $P\left((|\underline{h}_1|^2 - \bar{\gamma}_{th})^2 \leq (|\underline{h}_2|^2 + \bar{\gamma}_{th})^2\right)$, i.e. $P\left(|\underline{h}_1|^2 - |\underline{h}_2|^2 \leq 2\bar{\gamma}_{th}\right)$. It is known that, if $|\underline{h}_1|^2$ and $|\underline{h}_2|^2 \sim Exp(\lambda_u)$, then $W := |\underline{h}_1|^2 - |\underline{h}_2|^2$ is a RV following a double exponential distribution (or Laplace distribution), i.e., $W \sim Double - Exp(\lambda_u)$, with the PDF [47, eq.(2.2.8)], [44]

$$f_W(w) = \begin{cases} \frac{\lambda_u e^{\lambda_u w}}{2}, & w \leq 0; \\ \frac{\lambda_u e^{-\lambda_u w}}{2}, & w > 0. \end{cases} \tag{36}$$

Since the case $(s_1 \neq \acute{s}_1, s_2 = \acute{s}_2)$ occurs with the probability $P_{ij}(1 - P_{ij})$, the third component of the outage probability of the cooperative system, P_{03}^C, is upper

bounded by

$$P_{03}^{C} = P_{ij}(1-P_{ij})P(W \le 2\bar{\gamma}_{th}) = P_{ij}(1-P_{ij})\int_{-\infty}^{2\bar{\gamma}_{th}} f_W(w)dw = P_{ij}(1-P_{ij})\left[1-\frac{1}{2}e^{-\frac{2\bar{\gamma}_{th}}{\bar{\gamma}_u}}\right]. \quad (37)$$

- $\bar{\gamma}_{th} > 1$: In this case, one has

$$\gamma_c = \frac{|\underline{h}_1|^4}{|\underline{h}_2|^4 + 2|\underline{h}_1|^2 + 2|\underline{h}_2|^2} > \frac{|\underline{h}_1|^4}{|\underline{h}_2|^4 + 2\bar{\gamma}_{th}|\underline{h}_2|^2 + \bar{\gamma}_{th}^2 - \bar{\gamma}_{th} + 2|\underline{h}_2|^2} \quad (38)$$

Let us consider the inequality

$$\frac{|\underline{h}_1|^4}{(|\underline{h}_2|^2 + \bar{\gamma}_{th}|)^2 - \bar{\gamma}_{th} + 2|\underline{h}_2|^2} < \bar{\gamma}_{th} \quad (39)$$

Given that $\bar{\gamma}_{th} > 1$, after some simple manipulations, the above inequality is equivalent to

$$|\underline{h}_1|^2 - \sqrt{\bar{\gamma}_{th}}|\underline{h}_2|^2 < \bar{\gamma}_{th}(1+\bar{\gamma}_{th}). \quad (40)$$

$|\underline{h}_1|^2 - \sqrt{\bar{\gamma}_{th}}|\underline{h}_2|^2$ follows a double exponential distribution with the following PDF [48]

$$f_W(w) = \begin{cases} \frac{\lambda_u e^{\frac{\lambda_u w}{\sqrt{\bar{\gamma}_{th}}}}}{(1+\sqrt{\bar{\gamma}_{th}})}, & w \le 0; \\ \frac{\lambda_u e^{-\lambda_u w}}{(1+\sqrt{\bar{\gamma}_{th}})}, & w > 0. \end{cases} \quad (41)$$

Hence P_{03}^{C} in the case $\bar{\gamma}_{th} > 1$ is approximated by

$$P_{03}^{C} = P_{ij}(1-P_{ij})P(W < \bar{\gamma}_{th}(1+\bar{\gamma}_{th})) = P_{ij}(1-P_{ij})\int_{-\infty}^{\bar{\gamma}_{th}(1+\bar{\gamma}_{th})} f_W(w)dw = P_{ij}(1-P_{ij})\left[1-\frac{1}{1+\sqrt{\bar{\gamma}_{th}}}e^{-\frac{\bar{\gamma}_{th}(1+\sqrt{\bar{\gamma}_{th}})}{\bar{\gamma}_u}}\right]. \quad (42)$$

D. $s_1 \neq \acute{s}_1, s_2 \neq \acute{s}_2$

The instantaneous SNR is

$$\gamma_c = \frac{|\underline{h}_1|^4}{|\underline{h}_2|^4 + 2\left[1-\cos(\frac{2\pi}{M})\right]|\underline{h}_1|^2|\underline{h}_2|^2 + 2|\underline{h}_1|^2 + 2|\underline{h}_2|^2}. \quad (43)$$

Although Eq. (43) can be evaluated by replacing the RV $Z := |\underline{h}_1|^2|\underline{h}_2|^2$ by $\sqrt{\frac{3}{80}}(|\underline{h}_1|^2 + |\underline{h}_2|^2)$ as shown in Table 3, we notice that the case ($s_1 \neq \acute{s}_1, s_2 \neq \acute{s}_2$) occurs with a small probability P_{ij}^2. Thus, for simplicity, we can consider the following SNR value instead

$$\acute{\gamma}_c = \frac{|\underline{h}_1|^4}{\mathrm{E}\{|\underline{h}_2|^4 + 2\left[1-\cos(\frac{2\pi}{M})\right]|\underline{h}_1|^2|\underline{h}_2|^2 + 2|\underline{h}_1|^2 + 2|\underline{h}_2|^2\}} = \frac{|\underline{h}_1|^4}{2\bar{\gamma}_u\left[2+\bar{\gamma}_u\left(2-\cos(\frac{2\pi}{M})\right)\right]}. \quad (44)$$

We refer $\acute{\gamma}_c$ to as a quasi-instantaneous SNR value where the denominator is evaluated by its expectation value. It is worth noting that, deeply in its essence, the term "instantaneous SNR" in the literature, e.g., [36], [49], is also some type of quasi-instantaneous SNR because its denominator, i.e., the noise power, is also evaluated by its expectation value, which is σ^2. From (44), we have

$$P(\acute{\gamma}_c \le \bar{\gamma}_{th}) = P\left(|\underline{h}_1|^2 \le \sqrt{2\bar{\gamma}_{th}\bar{\gamma}_u\left[2+\bar{\gamma}_u\left(2-\cos\left(\frac{2\pi}{M}\right)\right)\right]}\right) = 1 - e^{-\sqrt{\frac{2\bar{\gamma}_{th}\bar{\gamma}_u\left[2+\bar{\gamma}_u\left(2-\cos\left(\frac{2\pi}{M}\right)\right)\right]}{\bar{\gamma}_u}}}, \quad (45)$$

where the last equality follows Eq. (22). The fourth component, P_{o4}^{C}, can be approximated as

$$P_{o4}^{C} \approx P_{ij}^2\left[1 - e^{-\sqrt{\frac{2\bar{\gamma}_{th}\bar{\gamma}_u\left[2+\bar{\gamma}_u\left(2-\cos\left(\frac{2\pi}{M}\right)\right)\right]}{\bar{\gamma}_u}}}\right]. \quad (46)$$

In summary, the closed approximation of the outage probability with M-PSK modulation is given in Eq. (47), as shown bottom of the next page.

Numerical formulas of all four outage components and the overall outage probability will be plotted against simulations in Section VII of this paper. Further, Eq. (47) will also be compared to the numerical outage probabilities of the direct transmission and the conventional Alamouti transmission (cf. Eqs. (24) and (25)) to evaluate the benefit of the cooperative communication.

V. ENERGY EFFICIENCY

We have analyzed numerically the cooperative system from the error performance and outage probability perspectives. Both numerical and simulated analyses reveal that the cooperation is better than the direct transmission in many cases. To quantify the fundamental limits of the cooperative system, in this section, we will analyze its Energy Efficiency (EE) defined as the ratio between the amount of successfully transmitted data, denoted as C (bits), and the total energy required to achieve that throughput, E_{total} (Joules). Note that, in the literature, EE can also be defined as the ratio between the system ergodic capacity (bits/s) and the consumed power (Watts) [50], [51], [52].

Let us denote L_p (bits) and L_d (bits) as the length of the whole packet and the length of payload data in each packet, respectively. Assume that a packet will be dropped if its Cyclic Redundancy Check (CRC) code fails. Denote R_b (bits/s) as the system bit rate and $b = \log_2(M)$ for a M-PSK modulation scheme, respectively.

From the symbol error rate, P_D, in Eq. (10) (or Eq. (19) for Rician channels), we can calculate the average Packet Error Rate (PER), denoted as $\overline{\mathrm{PER}}_D$, of the direct transmission scheme ($S_1 \rightarrow D$) as $\overline{\mathrm{PER}}_D = (1-P_D)^{L_p/b}$ [34], thus the effective throughput of the direct transmission is $C_D = L_d\overline{\mathrm{PER}}_D = L_d(1-P_D)^{L_p/b}$.

To calculate the total required energy, the component power model proposed by Cui *et al.* [53], where the total power consumption of a system is the sum of power consumptions of its components as shown in Fig. 3, will be considered. This model was proposed for a generic wireless link, so adaptations are needed for our considered cooperative system. The total power consumption can be written as $\mathcal{P}_{total} = \mathcal{P}_{pa} + \mathcal{P}_{ct} + \mathcal{P}_{cr} + \mathcal{P}_{bb}$, where $\mathcal{P}_{pa}$ is the amplifier power (PA) consumption (at the transmitter), $\mathcal{P}_{ct} = \mathcal{P}_{DAC} + \mathcal{P}_{mix} + \mathcal{P}_{filt} + \mathcal{P}_{syn}$ is the TX circuit power consumption (excluding both PA and the baseband processing power at the transmitter), $\mathcal{P}_{cr} = \mathcal{P}_{LNA} + \mathcal{P}_{filr} + \mathcal{P}_{mix} + \mathcal{P}_{syn} + \mathcal{P}_{IF} + \mathcal{P}_{ADC}$ is the RX circuit power consumption (excluding the baseband processing at the receiver), and $\mathcal{P}_{bb}$ is the baseband power consumption in both TX and RX, respectively. Notations $\mathcal{P}_{DAC}$, $\mathcal{P}_{mix}$, $\mathcal{P}_{filt}$, $\mathcal{P}_{syn}$, $\mathcal{P}_{LNA}$, $\mathcal{P}_{filr}$, $\mathcal{P}_{IF}$, and $\mathcal{P}_{ADC}$ denote the power consumption of the digital-to-analog converter, mixer, TX filter, synchronization, low-noise amplifier, RX filter, intermediate frequency processing, and analog-to-digital converter, respectively. Note that, except for the power consumption of the synchronization block which is assumed to be shared for all RF chains, other terms should be applied to each RF chain from a transmitter to a receiver. The values of these terms can be estimated by the model proposed in [53]. The PA consumption $\mathcal{P}_{pa}$ includes the actual transmitted power $\mathcal{P}_t$ and the wasteful power dissipation, thus $\mathcal{P}_{pa} = \frac{\mathcal{P}_t}{\eta}$, where η is the PA efficiency. The following EE analysis can be applied to both Rayleigh and Rician fading scenarios.

Consider the direct transmission with M-PSK modulation, one TX antenna, and n_R RX antennas. Energy required to transmit one packet with the data rate R_b (bits/s) will be

$$E^D_{total} = \frac{L_p}{R_b}\left(\frac{\mathcal{P}_t}{\eta} + \mathcal{P}_{ct} + n_R\mathcal{P}_{cr} + \mathcal{P}_{bb}\right). \quad (48)$$

Hence, EE of the direct transmission is

$$\begin{aligned} EE_D &= \frac{C_D}{E^D_{total}} \quad (bits/J) \\ &= \frac{R_b L_d}{L_p}\frac{(1-P_D)^{L_p/b}}{\left(\frac{\mathcal{P}_t}{\eta} + \mathcal{P}_{ct} + n_R\mathcal{P}_{cr} + \mathcal{P}_{bb}\right)}. \end{aligned} \quad (49)$$

To calculate EE of the cooperative system, for illustration, we will consider the half duplex scheme requiring three time slots (second scheme in Table 2), which is a typical scenario in WBANs. In the first (second) time slot, S_1 (S_2) broadcasts its own packet through its single TX antenna to n_R RX antennas of its partner as well as n_R RX antennas of the destination with the data rate R_b. The energy consumption in the first and second time slot can be approximated as

$$E_1 = E_2 \approx \frac{L_p}{R_b}\left(\frac{\mathcal{P}_t}{2\eta} + \mathcal{P}_{ct} + 2n_R\mathcal{P}_{cr} + 1.5\mathcal{P}_{bb}\right). \quad (50)$$

In Eq. (50), the factor $1/2$ of $\mathcal{P}_t$ reflects the fact that the signal power transmitted from each source node in one active time slot is half that power in the direct transmission. The factor $2n_R$ of $\mathcal{P}_{cr}$ is because the partner and the destination have total $2n_R$ RX antennas. The factor 1.5 of $\mathcal{P}_{bb}$ ($\mathcal{P}_{bb}$ is the baseband power consumption of one complete RF chain from TX to RX) approximates the power consumption of 'one and a half' complete RF chain, which includes the baseband processing blocks in a source node and those in

$$P_o^C = \begin{cases} (1-P_{ij})^2\left[1-\left(1+\frac{2\bar{\gamma}_{th}}{\bar{\gamma}_u}\right)e^{-\frac{2\bar{\gamma}_{th}}{\bar{\gamma}_u}}\right] + P_{ij}(1-P_{ij})\left[2- \right. \\ \left. \frac{1}{1+\sqrt{\bar{\gamma}_{th}}}e^{-\frac{\bar{\gamma}_{th}(1+\sqrt{\bar{\gamma}_{th}})}{\bar{\gamma}_u}}\right] + P_{ij}^2\left[1-e^{-\sqrt{\frac{2\bar{\gamma}_{th}\left[2+\bar{\gamma}_u\left(2-\cos\left(\frac{2\pi}{M}\right)\right)\right]}{\bar{\gamma}_u}}}\right], \quad \bar{\gamma}_{th} \geq \frac{\sqrt{\frac{20}{3}}}{\left[1-\cos\left(\frac{2\pi}{M}\right)\right]}; \\ (1-P_{ij})^2\left[1-\left(1+\frac{2\bar{\gamma}_{th}}{\bar{\gamma}_u}\right)e^{-\frac{2\bar{\gamma}_{th}}{\bar{\gamma}_u}}\right] + P_{ij}(1-P_{ij})\left[2- \right. \\ \left(1+\frac{2\bar{\gamma}_{th}}{\left(1-\sqrt{\frac{3}{20}}\left[1-\cos\left(\frac{2\pi}{M}\right)\right]\bar{\gamma}_{th}\right)\bar{\gamma}_u}\right)e^{-\frac{2\bar{\gamma}_{th}}{\left(1-\sqrt{\frac{3}{20}}\left[1-\cos\left(\frac{2\pi}{M}\right)\right]\bar{\gamma}_{th}\right)\bar{\gamma}_u}} \\ \left. -\frac{1}{1+\sqrt{\bar{\gamma}_{th}}}e^{-\frac{\bar{\gamma}_{th}(1+\sqrt{\bar{\gamma}_{th}})}{\bar{\gamma}_u}}\right] + P_{ij}^2\left[1-e^{-\sqrt{\frac{2\bar{\gamma}_{th}\left[2+\bar{\gamma}_u\left(2-\cos\left(\frac{2\pi}{M}\right)\right)\right]}{\bar{\gamma}_u}}}\right], \quad 1 < \bar{\gamma}_{th} < \frac{\sqrt{\frac{20}{3}}}{\left[1-\cos\left(\frac{2\pi}{M}\right)\right]}; \\ (1-P_{ij})^2\left[1-\left(1+\frac{2\bar{\gamma}_{th}}{\bar{\gamma}_u}\right)e^{-\frac{2\bar{\gamma}_{th}}{\bar{\gamma}_u}}\right] + P_{ij}(1-P_{ij})\left[2- \right. \\ \left(1+\frac{2\bar{\gamma}_{th}}{\left(1-\sqrt{\frac{3}{20}}\left[1-\cos\left(\frac{2\pi}{M}\right)\right]\bar{\gamma}_{th}\right)\bar{\gamma}_u}\right)e^{-\frac{2\bar{\gamma}_{th}}{\left(1-\sqrt{\frac{3}{20}}\left[1-\cos\left(\frac{2\pi}{M}\right)\right]\bar{\gamma}_{th}\right)\bar{\gamma}_u}} \\ \left. -\frac{1}{2}e^{-\frac{\bar{\gamma}_{th}}{\bar{\gamma}_u}}\right] + P_{ij}^2\left[1-e^{-\sqrt{\frac{2\bar{\gamma}_{th}\left[2+\bar{\gamma}_u\left(2-\cos\left(\frac{2\pi}{M}\right)\right)\right]}{\bar{\gamma}_u}}}\right], \quad \bar{\gamma}_{th} \leq 1; \end{cases} \quad (47)$$

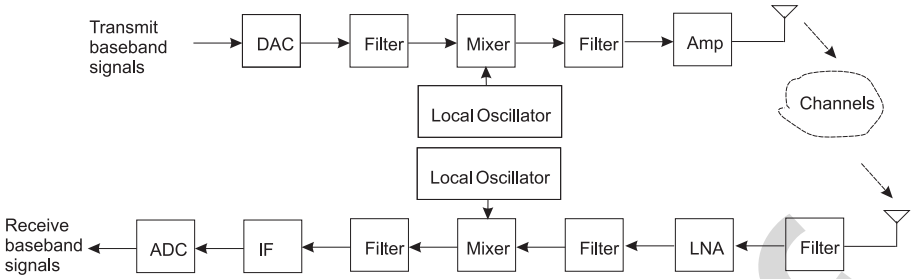

FIGURE 3. Component power model for energy efficiency analysis.

the destination (one complete RF chain) plus those in the receiving partner (roughly half a complete RF chain).

Similarly, the energy consumption in the third time slot can be approximated as

$$E_3 \approx \frac{L_p}{R_b}\left(\frac{\mathcal{P}_t}{\eta} + 2\mathcal{P}_{ct} + n_R\mathcal{P}_{cr} + 1.5\mathcal{P}_{bb}\right). \quad (51)$$

In Eq. (51), $\mathcal{P}_t$ does not have the factor 1/2 because S_1 and S_2 transmit simultaneously, which also explains the factor 2 of $\mathcal{P}_{ct}$. The factor n_R of $\mathcal{P}_{cr}$ indicates there is n_R RX antennas at the destination. The factor 1.5 of $\mathcal{P}_{bb}$ approximates the power consumption of the baseband processing blocks in the two transmitting nodes and in the destination. The total energy required to transmit two packets is the sum of E_1, E_2 and E_3, thus the average total energy required to transmit one packet of L_p bits will be

$$E^C_{total} = \frac{\sum_{j=1}^{3} E_j}{2} \approx \frac{L_p}{R_b}\left(\frac{\mathcal{P}_t}{\eta} + 2\mathcal{P}_{ct} + 2.5n_R\mathcal{P}_{cr} + 2.25\mathcal{P}_{bb}\right). \quad (52)$$

Consequently, EE of the cooperative communication system is

$$EE_C \approx \frac{R_b L_d}{L_p}\frac{(1-P_C)^{L_p/b}}{\left(\frac{\mathcal{P}_t}{\eta} + 2\mathcal{P}_{ct} + 2.5n_R\mathcal{P}_{cr} + 2.25\mathcal{P}_{bb}\right)}, \quad (53)$$

where P_C is calculated by Eq. (12) for Rayleigh fading channels, or Eq. (21) (with $\bar{\gamma}_{u1} = \bar{\gamma}_{u2}$) for Rician fading channels. Eqs. (48) and (52) reveal that the energies required for RF transmission in both direct transmission and cooperative communication are the same for a fair comparison as a result of our transmission schemes mentioned in Table 2, but the energies required for TX and RX circuits and baseband processing are slightly increased in the cooperative network.

The EE gain over the direct transmission is defined as

$$G_{EE} = \frac{EE_C}{EE_D} = \left(\frac{1-P_C}{1-P_D}\right)^{L_p/b} \times \left(\frac{\frac{\mathcal{P}_t}{\eta} + \mathcal{P}_{ct} + n_R\mathcal{P}_{cr} + \mathcal{P}_{bb}}{\frac{\mathcal{P}_t}{\eta} + 2\mathcal{P}_{ct} + 2.5n_R\mathcal{P}_{cr} + 2.25\mathcal{P}_{bb}}\right). \quad (54)$$

Note that P_D and P_C are functions of $\bar{\gamma}_{ij}$ and $\bar{\gamma}_u$, which are in turn calculated in dB as $\bar{\gamma}_{ij(u)} = 10\log_{10}(\mathcal{P}_t) - L_{ij(u)} - N_0 + (G_T + G_R - L_c)$, where $L_{ij(u)}$ denotes the pathloss of the internode link (uplink), N_0 is the noise power, and G_T, G_R, L_c denote the TX antenna gain, RX antenna gain, and total loss of connectors at both TX and RX antennas. For simplicity, we assume $(G_T + G_R - L_c)$ be the same for both internode links and uplinks. L_{ij} and L_u are functions of the distances d_{ij} and d_u, respectively. If internode links are the on-body to on-body communication links and the uplinks are the on-body to external links in WBANs, then L_{ij} can be estimated by the IEEE WBAN CM3 pathloss model while L_u follows the CM4 one [29].

The numerical evaluations in Eqs. (49), (53) and (54) will be plotted against the simulation results in Section VII of this paper.

VI. ASYMPTOTIC AND CLOSED-FORM ANALYSES

In this section, we will first derive the asymptotes of the SER curve of fully cooperative systems. Let us consider Eq. (7). When the uplink SNRs $\bar{\gamma}_{u1}$ and $\bar{\gamma}_{u2}$ are small, P_A is large. Thus P_A is a dominant component in Eq. (7). In other words, $P_C = P_A + 0.5(1-P_A)P_{ij} \gtrapprox P_A$. *This means P_A is the close lower bound of P_C in the lower-to-medium range of $\bar{\gamma}_{u1}$ and $\bar{\gamma}_{u2}$.*

On the other hand, by rewriting Eq. (7), we have $P_C = 0.5P_{ij} + P_A(1-0.5P_{ij}) \geq 0.5P_{ij}$. When $\bar{\gamma}_{u1}$ and $\bar{\gamma}_{u2}$ are large enough, P_A is negligible, i.e., the uplinks are error-free, thus $P_C = 0.5P_{ij}$. This formula is interpreted as follows. Information is broadcast from a source node (e.g., S_1) to the destination D and to its partner (S_2) first (see Table 2). The SER for the process $S_1 \rightarrow D$ is zero because this uplink is error-free. The internode link is however not error free if $\bar{\gamma}_{ij}$ is not large enough. Hence information arrives at S_2 with the SER P_{ij}. This information will be forwarded later by S_2 to D in the error-free uplink $S_2 \rightarrow D$. As a result, the average SER of the transmitted information is $P_C = \frac{0+P_{ij}}{2} = 0.5P_{ij}$. *Therefore $0.5P_{ij}$ is the close lower bound of P_C in the medium-to-large range of $\bar{\gamma}_{u1}$ and $\bar{\gamma}_{u2}$.*

So the SER curve of fully cooperative systems approaches the SER, P_A, of the Alamouti transmission in the lower-to-medium range of $\bar{\gamma}_{u1}$ and $\bar{\gamma}_{u2}$, and approaches half the SER of the internode links otherwise. These asymptotes will be confirmed later in Section VII.

Next we will derive mathematically the range of $\bar{\gamma}_{u1}$, $\bar{\gamma}_{u2}$ for a given $\bar{\gamma}_{ij}$ in which fully cooperative communication is

better than direct transmission, i.e., $P_C < P_D$, where P_D is the SER of the direct transmission from a source node to the destination (cf. Eq. (10)). For simplicity, let us consider the independently identically distributed Rayleigh fading channels, i.e., $\bar{\gamma}_{u1} = \bar{\gamma}_{u2} = \bar{\gamma}_u$. As mentioned above, when $\bar{\gamma}_u$ is large enough, $P_C \approx 0.5P_{ij}$, where P_{ij} is calculated by Eq. (9). Thus in order to find the range of $\bar{\gamma}_u$ in which fully cooperative communication is better than direct transmission, we have to solve the inequality $P_D > 0.5P_{ij}$.

It is known that the closed-form of

$$\frac{1}{\pi}\int_0^{(M-1)\pi/M}\left(1+\frac{\bar{\gamma}\sin^2(\pi/M)}{\sin^2(\phi)}\right)^{-n_R}d\phi,$$

is [36, eq.(9.42)]

$$\frac{1}{\left(4\bar{\gamma}\sin^2(\pi/M)\right)^{n_R}}\left[\binom{2n_R}{n_R}\frac{M-1}{M} - \sum_{n=1}^{n_R}\binom{2n_R}{n_R-n}(-1)^n\frac{\sin(2\pi n/M)}{n\pi}\right]. \quad (55)$$

From Eqs. (9), (10) and (55), it is easy to see that $P_D > 0.5P_{ij}$ is equivalent to

$$\frac{1}{\left(4\bar{\gamma}_u\sin^2(\pi/M)\right)^{n_R}} > 0.5\times\frac{1}{\left(4\bar{\gamma}_{ij}\sin^2(\pi/M)\right)^{n_R}},$$
$$\bar{\gamma}_u < \sqrt[n_R]{2}\,\bar{\gamma}_{ij}. \quad (56)$$

In other words, when $\bar{\gamma}_u$ is large enough, fully cooperative systems are better than direct transmission if $\bar{\gamma}_u$ (dB) $<$ $\bar{\gamma}_{ij}$ (dB) + $\frac{3}{n_R}$. In the special case $n_R = 1$, fully cooperative systems are always better than direct transmission from the error performance perspective if $\bar{\gamma}_u$ (dB) $<$ $\bar{\gamma}_{ij}$ (dB) + 3. This analysis will be confirmed by simulation results in Section VII.

Finally, we derive the closed-form of the SER of fully cooperative systems. By applying Eq. (55), the SER of fully cooperative systems in independently identically distributed Rayleigh fading channel shown in Eq. (12) has the closed-form given in Eq. (57), as shown at the bottom of this page.

VII. SIMULATION RESULTS AND DISCUSSIONS

Fig. 4 plots the SER (also BER), P_D, of the direct transmission system and, P_C, of the cooperative system, based on Eqs. (10) and (12), respectively, with $M = 2$ (BPSK) and $n_R = 1$ in identically distributed Rayleigh fading channels.

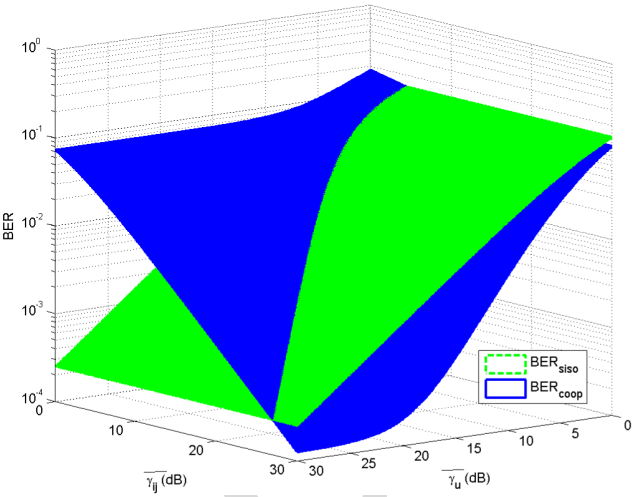

FIGURE 4. SER of the cooperative system as a function of both $\bar{\gamma}_{ij}$ and $\bar{\gamma}_u$ vs. SER of the direct transmission in BPSK modulation.

As shown in Eqs. (10) and (12), while P_D depends only on $\bar{\gamma}_u$, P_C is a bivariate function of both $\bar{\gamma}_{ij}$ and $\bar{\gamma}_u$. Fig. 4 shows clearly that, for a given $\bar{\gamma}_u$, when $\bar{\gamma}_{ij}$ increases to a certain value, the cooperative communication becomes better than the direct transmission which is indicated by the P_C surface going under the P_D surface. Unlike our intuition, the relation of $(\bar{\gamma}_{ij}, \bar{\gamma}_u)$ to make cooperative communication beneficial is not simply $\bar{\gamma}_{ij} > \bar{\gamma}_u$, but more complex as shown in Fig. 5, where the contour of the intersection between the P_D and P_C surfaces is the border between the area of useful cooperative communication (the crossed area) and the area where the direct transmission is better (the uncrossed area). As a matter of fact, the cooperative communication is better than the direct transmission even when $\bar{\gamma}_{ij} < \bar{\gamma}_u$, which can be seen clearly when the dotted line presenting the relation $\bar{\gamma}_{ij} = \bar{\gamma}_u$ is added as shown in this figure. Any point lying in the crossed area between this dotted line and the contour is corresponding to the case that the cooperative system is still better than the direct transmission although $\bar{\gamma}_{ij} < \bar{\gamma}_u$. From this figure, given two arbitrary SNR values $\bar{\gamma}_{ij}$ and $\bar{\gamma}_u$, one can also know whether the cooperative communication between S_1 and S_2 could be useful (if the point $(\bar{\gamma}_{ij}, \bar{\gamma}_u)$ is above the contour) or the direct transmission should be used instead. Fig. 5 also confirms our analysis in Section VI that, when $\bar{\gamma}_u$ is large enough, fully cooperative systems are always better than

$$P_C \approx \frac{1}{\left(2\bar{\gamma}_u\sin^2(\pi/M)\right)^{2n_R}}\left[\binom{4n_R}{2n_R}\frac{M-1}{M} - \sum_{n=1}^{2n_R}\binom{4n_R}{2n_R-n}(-1)^n\frac{\sin(2\pi n/M)}{n\pi}\right] + \frac{1}{2}\left\{1 - \frac{1}{\left(2\bar{\gamma}_u\sin^2(\pi/M)\right)^{2n_R}}\left[\binom{4n_R}{2n_R}\frac{M-1}{M} - \sum_{n=1}^{2n_R}\binom{4n_R}{2n_R-n}(-1)^n\frac{\sin(2\pi n/M)}{n\pi}\right]\right\}\times \frac{1}{\left(4\bar{\gamma}_{ij}\sin^2(\pi/M)\right)^{n_R}}\left[\binom{2n_R}{n_R}\frac{M-1}{M} - \sum_{n=1}^{n_R}\binom{2n_R}{n_R-n}(-1)^n\frac{\sin(2\pi n/M)}{n\pi}\right]. \quad (57)$$

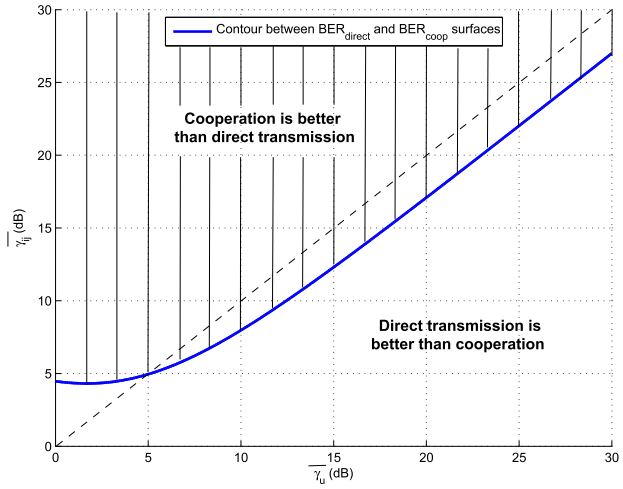

FIGURE 5. Coordinates ($\bar{\gamma}_{ij}$, $\bar{\gamma}_u$) where cooperative communication is useful (BPSK modulation, $n_R = 1$).

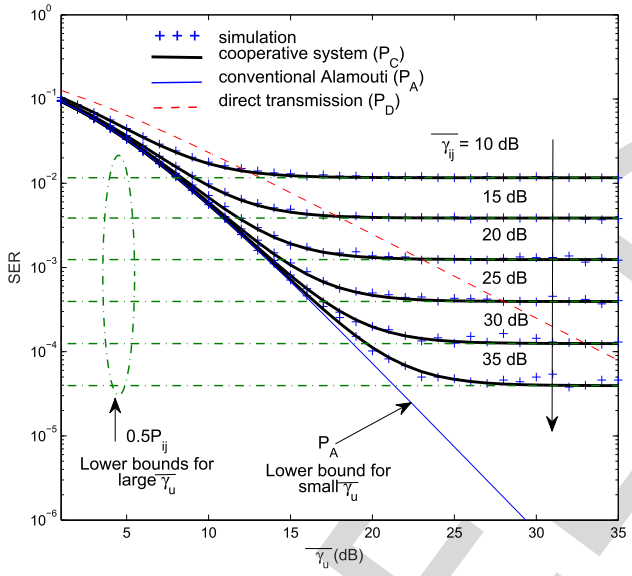

FIGURE 6. Error performances of the direct transmission system, cooperative system, and conventional Alamouti system with BPSK, $n_R = 1$, and identically distributed Rayleigh fading channels. Solid and dashed curves show the numerical analysis, while plus sign markers show the simulations.

direct transmission from the error performance perspective if $\bar{\gamma}_u$ (dB) $< \bar{\gamma}_{ij}$ (dB) + 3.

To examine Fig. 4 more closely, we consider a fixed value $\bar{\gamma}_{ij}$ while varying $\bar{\gamma}_u$. The SERs P_D and P_C in Eqs. (10) and (12), respectively, can be presented in a two dimensional Cartesian coordinate as shown in Fig. 6. For comparison, we also plot SERs of the direct transmission and the conventional Alamouti code. From Fig. 6, we have four observations. First, the simulated SER curves fit very well the numerical SERs calculated by Eqs. (10) and (12), which confirms the validity of our theoretical analysis. Second, the cooperative system is better than the direct transmission provided that $\bar{\gamma}_u$ (dB) $< \bar{\gamma}_{ij}$ (dB) + 3, which confirms our analysis in Section VI. Third, the performance of the fully cooperative system approaches that of the conventional Alamouti code in the lower-to-medium range of $\bar{\gamma}_u$ and approaches $0.5P_{ij}$ in the medium-to-high range of $\bar{\gamma}_u$, which confirm our analysis on the asymptotes in Section VI. Hence the cooperative system approaches the full diversity order. Note that, unlike in a conventional MIMO system, diversity order of the cooperative system is also a bivariate function of both $\bar{\gamma}_{ij}$ and $\bar{\gamma}_u$. Hence, the terminology "diversity order" need to be clearly defined. In this paper, we refer diversity order of the cooperative system to as the slope of the SER curve with respect to $\bar{\gamma}_u$, given a certain value of $\bar{\gamma}_{ij}$. of two (as the Alamouti code) at a lower range of $\bar{\gamma}_u$, which is an attractive property of the cooperative communication. Fourth, for a certain $\bar{\gamma}_{ij}$, there is no point to keep increasing $\bar{\gamma}_u$ as, to a certain point of $\bar{\gamma}_u$, the performance of the cooperative system will be saturated, thus the direct transmission starts to be better than the cooperative communication. This saturation does not appear in the conventional Alamouti code, which does not involve in the information exchange between S_1 and S_2. This saturation is explained by the fact that, in the cooperative communication, a large value of $\bar{\gamma}_u$ almost nullifies the component P_A in Eq. (12), thus SER of the cooperative communications no longer depends on $\bar{\gamma}_u$. With the terminology "diversity order" defined in the footnote, diversity order of the cooperative system changes from two (full diversity) in a lower range of $\bar{\gamma}_u$ to zero in its higher range. It is worth noting that typical WBAN applications work at low SNRs as detailed in Section I, making the cooperative system especially attractive.

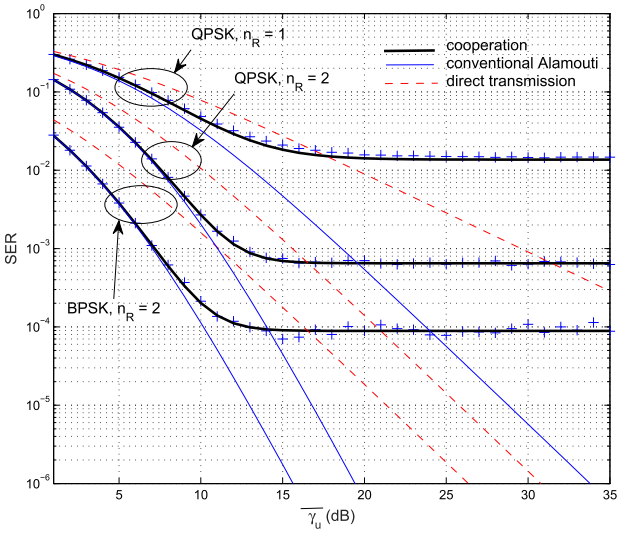

FIGURE 7. Error performances of three systems with BPSK and QPSK, one or two RX antennas, and identically distributed Rayleigh fading channels. Thick black solid curves - cooperative communication, blue solid curves with circle markers - conventional Alamouti transmission, and dashed curves - direct transmission.

Comparing with the direct transmission and the conventional Alamouti transmission, similar observations for the error performance gain and the diversity order of the cooperative system can be drawn from Fig. 7, where SER of the

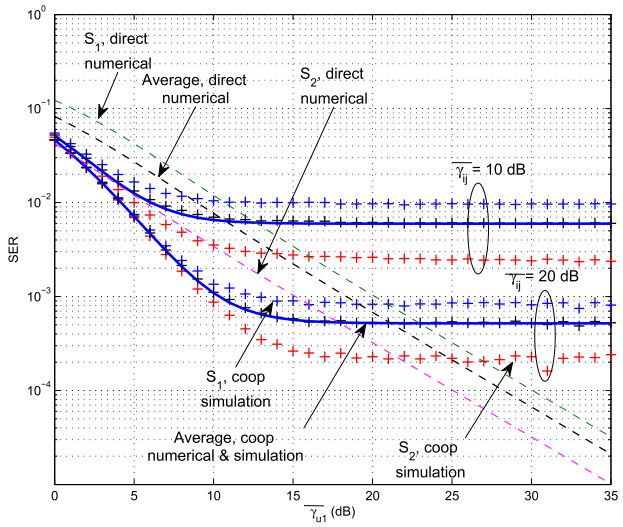

FIGURE 8. SER of the cooperative system in non-identically distributed Rician channels with BPSK, $n_R = 1$, $K_1 = K_2 = 2$, $\bar{\gamma}_{ij} = 10$ and 20 dB, $\bar{\gamma}_{u2} = \bar{\gamma}_{u1} + 5$ dB. Plus markers indicate simulation results.

cooperative system with a higher modulation scheme (QPSK) and with multiple RX antennas per node is plotted. The cooperative system approaches the full diversity order of four if each node is equipped with $n_R = 2$ RX antennas at a lower range of $\bar{\gamma}_u$, i.e., SER reduces roughly 100 times when $\bar{\gamma}_u$ increases by 5 dB. From Fig. 7, it is clear that having multiple RX antennas magnifies the benefit of the cooperative communication.

Fig. 8 presents SER of the cooperative system versus SER of the direct transmission in non-identically distributed Rician channels. To create the non-identically distributed Rician channels, we assume that the Rician factors of two uplinks from S_1 and S_2 to D are the same, i.e., $K_{u1} = K_{u2} = 2$, but their average SNRs follow the relation $\bar{\gamma}_{u2} = \bar{\gamma}_{u1} + 5$ dB. An example of non-identically distributed channels is when one of the two sensors is persistently impeded by obstacles, such as an identity card, in a patient's pocket. Individual SERs of S_1 and S_2 as well as their average SER are plotted against those of the direct transmission from each node to the destination used as the benchmarks. The curves with plus sign markers indicate the simulated SERs, while other curves are plotted based on our numerical analysis (cf. Eqs. (19) and (21)). Two interesting observations can be drawn from Fig. 8. First, the error performance of each individual node will be better than its own direct transmission at a low-to-medium SNR range if the node cooperates with its partner. Second, the average error performance of the two nodes in the cooperative system is not only better than the error performance averaged over the two direct transmissions, but may also be better than the best direct transmission performance among the two nodes at a low-to-medium SNR range if the internode links are good enough (i.e., $\bar{\gamma}_{ij} = 20$ dB in this example). It is worth noting that two source nodes here can be considered as two different users in a more general multi-user WSN/WBAN scenario.

TABLE 4. Parameters for simulations of energy efficiency.

Parameters	Values
PA efficiency	$\eta = 35\%$ [53], [50], [51], [52]
Transmission power	$\mathcal{P}_t = 200$ nW [54] (if d_u fixed)
Circuit power	$\mathcal{P}_{ct} = 100$ nW, $\mathcal{P}_{cr} = 80$ nW [54]
Baseband power	$\mathcal{P}_{bb} = 50$ nW [54]
Frequency	900 MHz [29, p.7]
Bandwidth	25 MHz
Data rate	$R_b = 1$ Mbps
$G_T + G_R - L_c$	2 dB
Packet length	$L_p = 56$ bits [34]
Payload length	$L_d = 40$ bits [34]
Modulation	BPSK or QPSK
PSD of noise	-174 dBm/Hz [53]
Pathloss model	IEEE WBAN model [29]
	Internode - CM3, uplinks - CM4
Distances	$d_{ij} = 0.3$ m
	$d_u = 0.1 - 10$ m [29] (if $\mathcal{P}_t$ fixed)

Figs. 9 and 10 present the numerical and simulated curves of all four outage probability components (cf. Eqs. (29), (33), (42), (46) and of the overall outage probability (cf. Eq. (47) for BPSK of the cooperative system as functions of the ratio $\frac{\bar{\gamma}_{th}}{\bar{\gamma}_u}$. The outage probabilities of the direct transmission (cf. Eq. (24)) and of the conventional Alamouti transmission (cf. Eq. (25)) are also plotted for comparison. Fig. 9 illustrates the case where both $\bar{\gamma}_{ij}$ and $\bar{\gamma}_u$ are varied but equal each other, while Fig. 10 considers a fixed $\bar{\gamma}_{ij}$ value (here $\bar{\gamma}_{ij} = 10$ dB) but $\bar{\gamma}_u$ is varied. From these figures, we have the following observations. First, the simulated outage probability components and the simulated overall outage probability, presented by the curves with plus sign markers, are well approximated by the numerical outage probabilities mentioned in Eqs. (29), (33), (42), (46), and (47) in both linear and logarithmic scales. Second, the outage probability of the cooperative system approaches that of the conventional Alamouti system, especially at a medium-to-high range of $\frac{\bar{\gamma}_{th}}{\bar{\gamma}_u}$, i.e., at a low-to-medium range of $\bar{\gamma}_u$ since $\bar{\gamma}_{th}$ is an arbitrary fixed value ($\bar{\gamma}_{th} = 5$ dB was simulated for both figures). Consistently with the SER performance, when $\bar{\gamma}_{ij}$ is fixed and $\bar{\gamma}_u$ keeps increasing to a certain point (i.e., $\frac{\bar{\gamma}_{th}}{\bar{\gamma}_u}$ is small enough), the outage probability of the cooperative system starts to be worse than the direct transmission. Third, at very low $\bar{\gamma}_u$ values, the direct transmission is slightly better than the conventional Alamouti code (but worse than the Alamouti transmission from the error performance perspective). This is because the transmitted power per TX antenna in the Alamouti code is only half that power in the direct transmission. This is why outage probabilities should also be considered to evaluate the MIMO performance, in addition to the SER performance. From Fig. 10, clearly, the cooperative system is better than the direct transmission within the range $\frac{\bar{\gamma}_{th}}{\bar{\gamma}_u} \in [-14, 1]$ dB, i.e., $\bar{\gamma}_u \in [4, 19]$ dB from the outage perspective. Note that $\bar{\gamma}_{ij} = 10$ dB. Meanwhile, from the error performance perspective, the cooperative system is better than the direct transmission provided that $\bar{\gamma}_u \leq 13$ dB as shown in Fig. 6. This means the cooperative system is better than the direct transmission within the range $\bar{\gamma}_u \in [4, 13]$ dB from both perspectives.

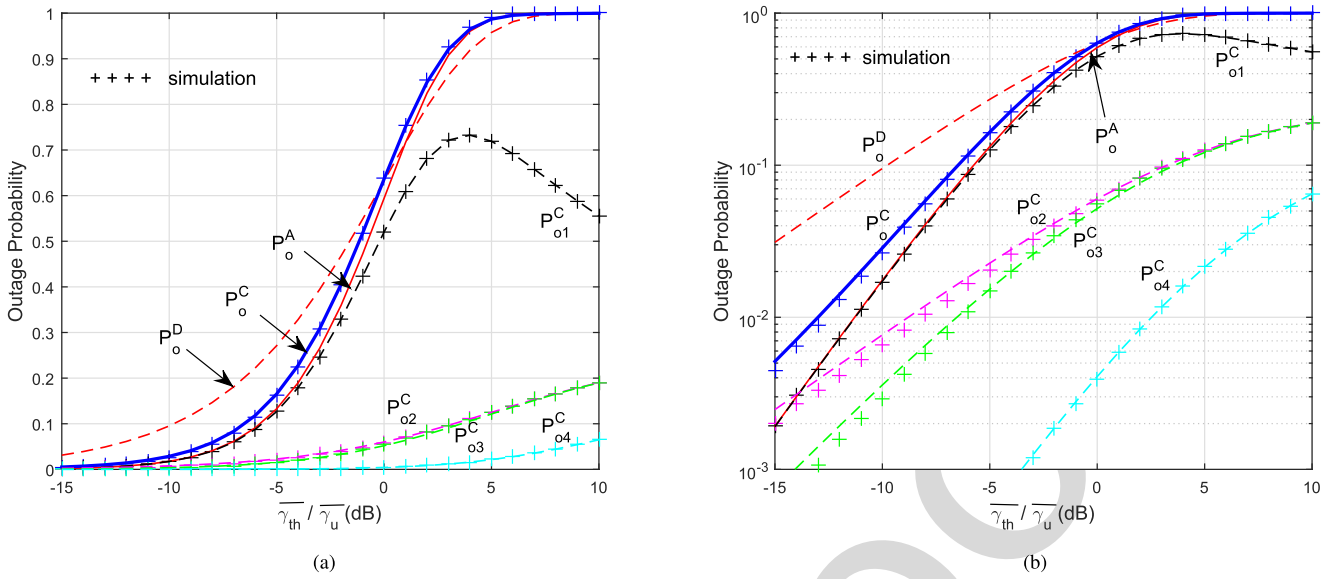

FIGURE 9. Component outage probabilities and overall outage probability of the cooperative system vs. outage of direct transmission and of the Alamouti transmission, assuming $\bar{\gamma}_{ij} = \bar{\gamma}_u$. Solid curves and dashed curves show the numerical analysis, while plus sign markers indicate the simulation results. (a) Linear scale. (b) Logarithmic scale.

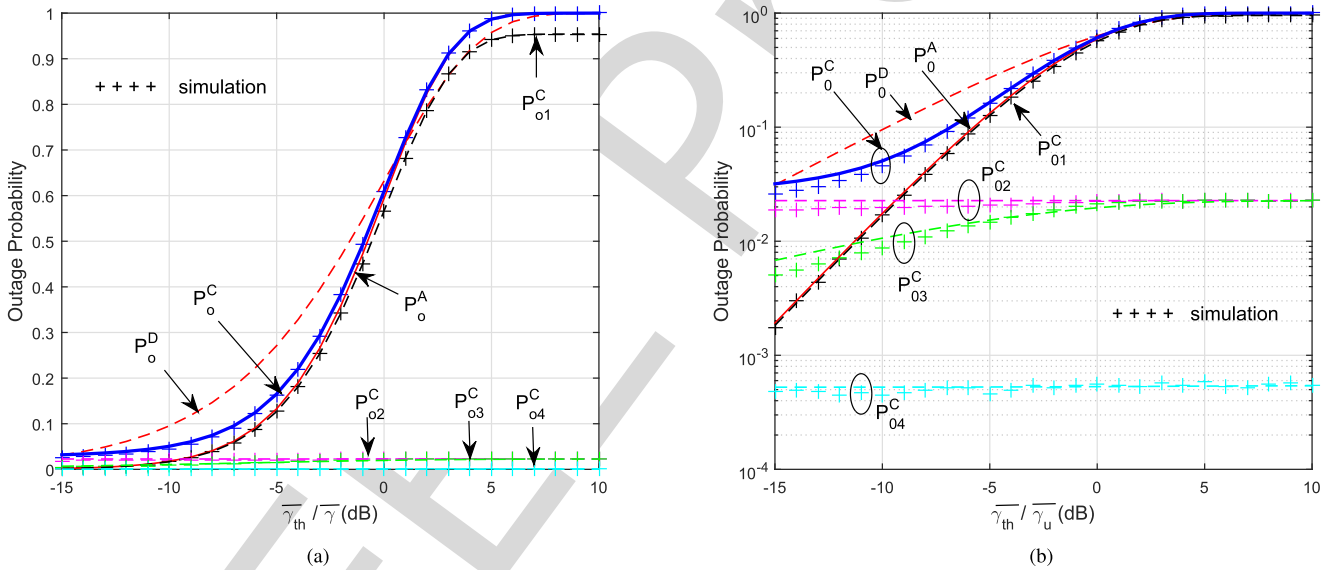

FIGURE 10. Component outage probabilities and overall outage probability of the cooperative system vs. outage of direct transmission and of the Alamouti transmission, assuming $\bar{\gamma}_{ij} = 10$ dB. Solid curves and dashed curves show the numerical analysis, while plus sign markers indicate the simulation results. (a) Linear scale. (b) Logarithmic scale.

To evaluate EE of the cooperative communication, we consider the simulation parameters listed in Table 4. It is worth noting that, due to the lack of available power specifications of realistic hardware in WBANs at 900 MHz, in Table 4, we have assumed the values of $\mathcal{P}_t$, $\mathcal{P}_{ct}$ (or $\mathcal{P}_{cr}$), and $\mathcal{P}_{bb}$ to follow roughly the ratio 4:2:1 as shown in [54, p.26] for practical hardware in WSNs at 868 MHz, and that the actual radio hardware transmitting as low as some hundreds nW has been reported in the literature, such as [55]. Fig. 11(a) presents the numerical EE of the cooperative system (cf. Eq. (53)), indicated by the solid curves, and of the direct transmission system (cf. Eq. (49)), indicated by the dashed curves, in both $n_R = 1$ and $n_R = 2$ scenarios with either BPSK or QPSK. This figure shows EE as a function of the distance d_u from the sources to the destination, which could be up to 10 m for a typical WBAN application. The simulated EE of the two systems are also plotted to confirm the validity of Eqs. (49) and (53). Meanwhile, Fig. 11(b) presents the numerical EE gain (cf. Eq. (54)) achieved by the cooperative system over the direct transmission. One can see from Fig. 11(b) that the EE gain achieved by the cooperative system is more significant when $n_R = 1$. This is due to the fact that a

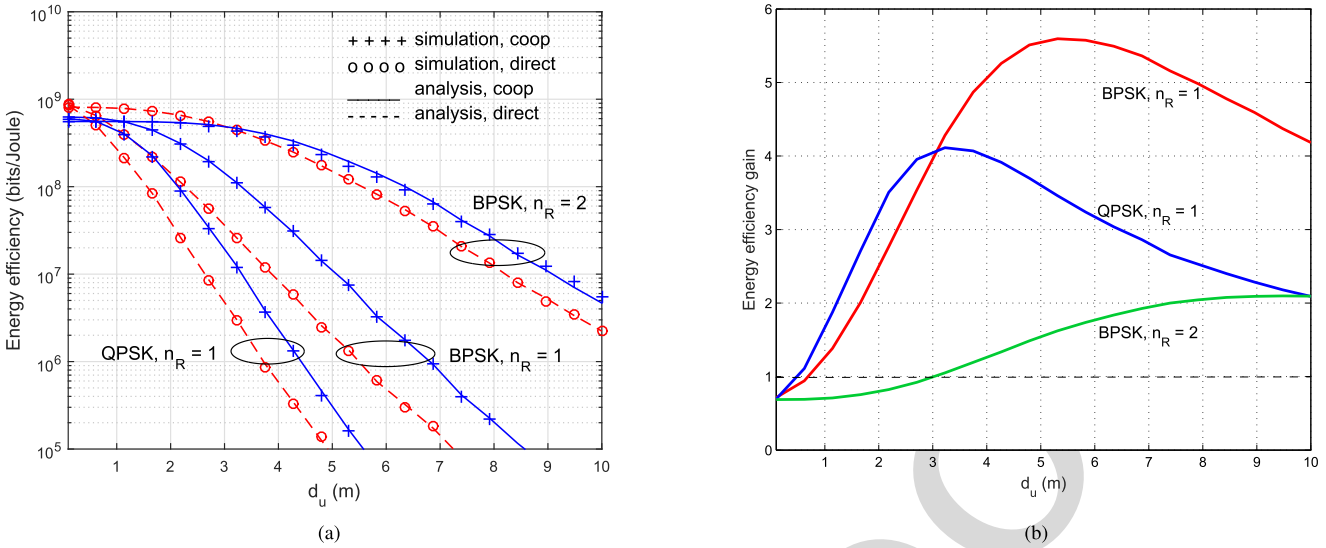

FIGURE 11. Numerical and simulated *EE* and G_{EE} of the cooperative communication versus those in the direct transmission. (a) *EE*. (b) G_{EE}.

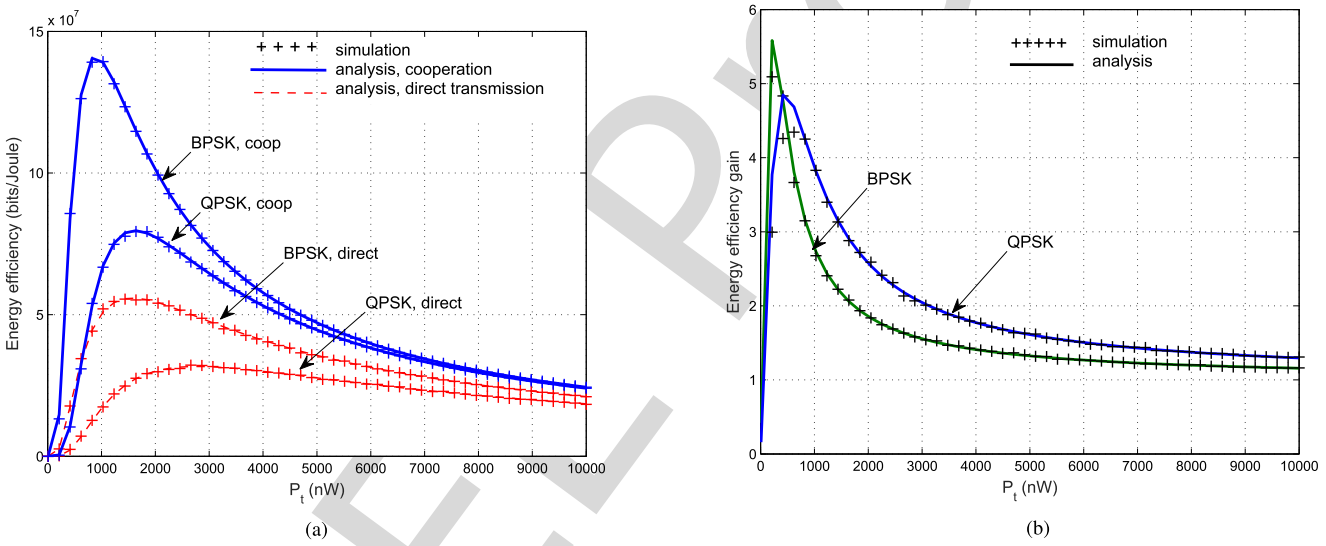

FIGURE 12. Numerical and simulated *EE* and G_{EE} as functions of the transmitted power $\mathcal{P}_t$ in the cooperative communication and in the direct transmission. (a) *EE*. Dashed curves - direct transmission, solid - cooperation. Circle markers - BPSK, $n_R = 1$; square - BPSK, $n_R = 2$. Plus markers - simulated cooperation, asterisks - simulated direct transmission. (b) G_{EE}.

multiple RX antenna system already achieves a certain EE gain by the MIMO configuration even without cooperation. Fig. 11 shows clearly that the cooperative system provides a slightly smaller EE, compared to the direct transmission, when the destination is near to the source nodes (within 0.7 m for $n_R = 1$), but it can provide a much larger EE at further distances, i.e., at a lower range of the uplink SNR ($\bar{\gamma}_u <$ 15.72 dB for $n_R = 1$). This is another attractive feature of the cooperative system, especially when $n_R = 1$, since the distance from the sources to an external hub usually exceeds one meter in a typical WBAN application. Also this uplink SNR range covers the $\bar{\gamma}_u$ range [4, 13] dB stated earlier from the SER and outage probability perspectives. In other words, the cooperative communication could be better than the direct transmission within the range $\bar{\gamma}_u \in [4, 13]$ dB from all three (error performance, outage probability and energy efficiency) perspectives.

Fig. 12(a) presents the numerical EE of the cooperative system (solid curves) in comparison with the numerical EE of the direct transmission (dashed) as a function of the transmission power $\mathcal{P}_t$ with $n_R = 1$ and with either BPSK or QPSK modulation. Simulation parameters have been mentioned in Table 4. Fig. 12(b) shows the corresponding EE gain. The simulated EE and gain are also plotted in both figures, which match really well the numerical EE and gains. One interesting observation drawn from these figures is, while the

cooperative communication system has a better EE than the direct transmission for the whole range of the transmission power considered in this simulation, it is extremely useful, compared to the direct transmission, at the lower transmission power regime of few microwatts. This feature is very useful for WBAN applications where the maximum transmission power is regulated by rigorous regulations. For instance, the maximum power limitation for medical implant communication services is set to $15.24\mu W$ EIRP by the ETSI as mentioned earlier in Section I.

VIII. CONCLUSION

In this paper, we have derived for the first time the exact numerical SER formulas for a three-node decode-and-forward, space-time coded, fully cooperative communication network in both Rayleigh and Rician fading channels with M-PSK modulation in either identically or non-identically distributed branch scenario. We have derived the closed forms of the system outage probabilities of three systems, namely the direct transmission, the conventional Alamouti transmission and the cooperative system, in identically distributed Rayleigh fading channels with M-PSK modulation. Finally, the energy efficiencies of these three systems have been analyzed in both Rayleigh and Rician fading conditions. Throughout the paper, simulation results have been shown to match well the numerical results, thus verifying our theoretical analysis. The numerical analysis and simulation results have proved that the cooperative communication system is better then the direct transmission in many cases, especially at a low power, low SNR regime, which is a typical working condition of WBANs, from all error performance, outage, and energy efficiency perspectives. This proof is a novel contribution of this paper, providing comprehensive answers to the commonly asked questions of whether, when and to what extent the cooperative communication could be useful from the three perspectives, hence putting one more milestone to the perception process of generic cooperative communication systems. Inspired by WBAN systems, our analysis is also readily applied to generic Rayleigh and Rician wireless channels, such as in wireless IoT and indoor entertainment applications. This paper has analyzed the flat fading Rayleigh and Rician wireless channels. Due to the limited space, our analysis of the cooperative communication system in frequency selective fading channels using the OFDM technique will be mentioned in another paper.

The paper has considered both identically and non-identically distributed independent fading channels between nodes. In WBANs, nodes possibly experience temporal and spatial correlations. For instance, when one sensor located on a wrist or thigh and the other sensor located on the hip of a walking person may have a spatial correlation coefficient within the range [- 0.5, 0.7] as pointed out in [56]. Research of fully cooperative communication in spatially correlated WBAN fading channels is of our interest. Further, while this paper has considered flat Rayleigh and Rician channels, which are applicable to the narrow bands of the on-body to on-body (CM3) and on-body to external (CM4) links [29], it has not considered log-normal channels which have been shown to be present in the UWB bands of WBANs [29]. Performance analysis of fully cooperative communication systems for UWB bands is our future work.

REFERENCES

[1] A. Sendonaris, E. Erkip, and B. Aazhang, "User cooperation diversity. Part I. System description," *IEEE Trans. Commun.*, vol. 51, no. 11, pp. 1927–1938, Nov. 2003.
[2] A. Nosratinia, T. E. Hunter, and A. Hedayat, "Cooperative communication in wireless networks," *IEEE Commun. Mag.*, vol. 42, no. 10, pp. 74–80, Oct. 2004.
[3] T. E. Hunter and A. Nosratinia, "Diversity through coded cooperation," *IEEE Trans. Wireless Commun.*, vol. 5, no. 2, pp. 283–289, Feb. 2006.
[4] S. Alamouti, "A simple transmit diversity technique for wireless communications," *IEEE J. Sel. Areas Commun.*, vol. 16, no. 8, pp. 1451–1458, Oct. 1998.
[5] L. C. Tran, T. A. Wysocki, A. Mertins, and J. Seberry, *Complex Orthogonal Space-Time Processing in Wireless Communications*. New York, NY, USA: Springer, 2006.
[6] J. N. Laneman, D. N. C. Tse, and G. W. Wornell, "Cooperative diversity in wireless networks: Efficient protocols and outage behavior," *IEEE Trans. Inf. Theory*, vol. 50, no. 12, pp. 3062–3080, Dec. 2004.
[7] N. C. Beaulieu and J. Hu, "A closed-form expression for the outage probability of decode-and-forward relaying in dissimilar Rayleigh fading channels," *IEEE Commun. Lett.*, vol. 10, no. 12, pp. 813–815, Dec. 2006.
[8] J. He and P. Y. Kam, "Exact bit error probability of cooperative space-time block coding with amplify-and-forward strategy," in *Proc. IEEE Int. Conf. Commun. (ICC)*, May 2008, pp. 4591–4595.
[9] P. Huo and L. Cao, "Distributed STBC with soft information relay based on Gaussian approximation," *IEEE Signal Process. Lett.*, vol. 19, no. 10, pp. 599–602, Oct. 2012.
[10] K. Tourki, M.-S. Alouini, and H.-C. Yang, "Exact performance analysis of decode-and-forward opportunistic relaying," in *Proc. 11th IEEE Int. Workshop Signal Process. Adv. Wireless Commun. (SPAWC)*, Jul. 2010, pp. 1–5.
[11] Q. Shi and Y. Karasawa, "Error probability of opportunistic decode-and-forward relaying in Nakagami-m fading channels with arbitrary m," *IEEE Wireless Commun. Lett.*, vol. 2, no. 1, pp. 86–89, Feb. 2013.
[12] K. Ho-Van, "Performance analysis of cooperative underlay cognitive networks with channel estimation error," *Wireless Pers. Commun.*, vol. 77, no. 4, pp. 2687–2697, 2014.
[13] A. I. Akın, H. Ilhan, and O. Özdemir, "Error performance analysis of decode and forward based cooperative systems with relay selection," in *Proc. 21st IEEE Sign. Process. Commun. Appl. Conf. (SIU)*, Apr. 2013, pp. 1–4.
[14] A. Karademir, and I. Altunbaş, "Error performance of cooperative systems in generalized-K channels," in *Proc. 21st IEEE Signal Process. Commun. Appl. Conf. (SIU)*, Apr. 2013, pp. 1–4.
[15] D. Wang and L. Hao, "Performance analysis for cooperative relay communication," *Wireless Pers. Commun.*, vol. 71, no. 3, pp. 1619–1631, Aug. 2013.
[16] S. Silva, G. Amarasuriya, C. Tellambura, and M. Ardakani, "Relay selection strategies for MIMO two-way relay networks with spatial multiplexing," *IEEE Trans. Commun.*, vol. 63, no. 12, pp. 4694–4710, Dec. 2015.
[17] A. H. A. El-Malek and S. A. Zummo, "A bandwidth-efficient cognitive radio with two-path amplify-and-forward relaying," *IEEE Wireless Commun. Lett.*, vol. 4, no. 1, pp. 66–69, Feb. 2015.
[18] M. Hussain and S. A. Hassan, "Performance of multi-hop cooperative networks subject to timing synchronization errors," *IEEE Trans. Commun.*, vol. 63, no. 3, pp. 655–666, Mar. 2015.
[19] A. Afana, R. Mesleh, S. Ikki, and I. E. Atawi, "Performance of quadrature spatial modulation in amplify-and-forward cooperative relaying," *IEEE Commun. Lett.*, vol. 20, no. 2, pp. 240–243, Feb. 2016.
[20] A. A. Nasir, D. T. Ngo, X. Zhou, R. A. Kennedy, and S. Durrani, "Joint resource optimization for multicell networks with wireless energy harvesting relays," *IEEE Trans. Veh. Technol.*, vol. 65, no. 8, pp. 6168–6183, Aug. 2016.
[21] Y. Luo, J. Zhang, and K. B. Letaief, "Transmit power minimization for wireless networks with energy harvesting relays," *IEEE Trans. Commun.*, vol. 64, no. 3, pp. 987–1000, Mar. 2016.

[22] K. M. Rabie, A. Salem, E. Alsusa, and M. S. Alouini, "Energy-harvesting in cooperative AF relaying networks over log-normal fading channels," in *Proc. IEEE Int. Conf. Commun. (ICC)*, May 2016, pp. 1–7.

[23] M. M. Alam, and E. B. Hamida, "Surveying wearable human assistive technology for life and safety critical applications: Standards, challenges and opportunities," *Sensors*, vol. 14, no. 5, pp. 9153–9209, 2014.

[24] European Commission. (2010). *Wiser BAN—Smart Miniature Low-Power Wireless Microsystem for Body Area Networks*. [Online]. Available: http://www.wiserban.eu/

[25] European Union. (2010). *Wear-a-BAN—Unobtrusive Wearable Human to Machine Wireless Interface*. [Online]. Available: http://www.wearaban.com/

[26] M. H. Rehmani, E. Ahmed, S. U. Khan, and M. Radenkovic, "IEEE Access special section editorial: Body area networks for interdisciplinary research," *IEEE Access*, vol. 4, pp. 2989–2992, Jul. 2016.

[27] L. C. Tran, Z. Lin, F. Safaei, A. Mertins, and N. T. Duy, "Exact error performance analysis of binary space-time block coded cooperative communications systems in Rayleigh fading channels," in *Proc. IEEE Int. Conf. Adv. Technol. Commun. (ATC)*, Oct. 2015, pp. 567–571.

[28] L. C. Tran and A. Mertins, "Error performance and energy efficiency analyses of fully cooperative OFDM communication in frequency selective fading," *IET Commun.*, vol. 10, no. 18, pp. 1–9, Oct. 2016.

[29] K. Y. Yazdandoost and K. Sayrafian-Pour, "Channel model for body area network (BAN)," IEEE Standards Assoc., Piscataway, NJ, USA, Tech. Rep. IEEE 802.15-08-0780-12-0006, Nov. 2010.

[30] D. Smith, L. Hanlen, J. Zhang, D. Miniutti, D. Rodda, and B. Gilbert, "First- and second-order statistical characterizations of the dynamic body area propagation channel of various bandwidths," *Ann. Telecommun.*, vol. 66, no. 3, pp. 187–203, 2011.

[31] *Report and Order (FCC 09-23)*, FCC, Mar. 2009.

[32] CEPT70-03. (Aug. 2011). *ERC Recommendation 70-03 (Tromso 1997 and Subsequent Ammendments) Relating to the Use of Short Range Device (SRD) (ERC/REC 70-03)*. [Online]. Available: http://www.cept.org/Documents/srd/mg/933/Info_6_ERC_REC_70-03_August_2011.

[33] *Report and Order (FCC 96-326)*, FCC, Aug. 1996.

[34] S. Wang and J. Nie, "Energy efficiency optimization of cooperative communication in wireless sensor networks," *EURASIP J. Wireless Commun. Netw.*, vol. 2010, pp. 1–8, Apr. 2010.

[35] H. Feng, B. Liu, Z. Yan, C. Zhang, and C. W. Chen, "Prediction-based dynamic relay transmission scheme for wireless body area networks," in *Proc. IEEE 24th Int. Symp. Personal Indoor Mobile Radio Commun. (PIMRC)*, Sep. 2013, pp. 2539–2544.

[36] M. K. Simon and M.-S. Alouini, *Digital Communication Over Fading Channels: A Unified Approach to Performance Analysis*. New York, NY, USA: Wiley, 2000.

[37] W. Abbott *et al.* (Aug. 2009). *Multiband OFDM Physical Layer Specification*. [Online]. Available: http://www.wimedia.org/en/docs/10003r02WM_CRB-WiMedia_PHY_Spec_1.5.pdf

[38] L. C. Tran, A. Mertins, and T. A. Wysocki, "Cooperative communication in space-time-frequency coded MB-OFDM UWB," in *Proc. IEEE 68th Veh. Technol. Conf. (VTC)*, Sep. 2008, pp. 1–5.

[39] Z. Lin, L. C. Tran, and F. Safaei, "Order-4 orthogonal cooperative communication in space-time-frequency coded MB-OFDM UWB," in *Proc. Int. Symp. Commun. Inf. Technol. (ISCIT)*, Oct. 2012, pp. 920–925.

[40] A. Maaref and S. Aissa, "Performance analysis of orthogonal space-time block codes in spatially correlated MIMO Nakagami fading channels," *IEEE Trans. Wireless Commun.*, vol. 4, no. 5, pp. 807–817, Apr. 2006.

[41] A. Müller and J. Speidel, "Orthogonal STBC in general Nakagami-m fading channels: BER analysis and optimal power allocation," in *Proc. 65th IEEE Veh. Technol. Conf. (VTC)*, Apr. 2007, pp. 1698–1702.

[42] F. Xu and D.-W. Yue, "Exact error probability of orthogonal space-time block codes over fading channels," in *Proc. 6th IEEE Int. Conf. Telecommmun. (ITS)*, Sep. 2006, pp. 469–472.

[43] P. J. Lee, "Computation of the bit error rate of coherent M-ary PSK with Gray code bit mapping," *IEEE Trans. Commun.*, vol. COM-34, no. 5, May 1986.

[44] R. Adve. (May 2007). *Diversity Receive*. [Online]. Available: http://www.comm.utoronto.ca/~rsadve/Notes/DiversityReceive.pdf

[45] N. J. Redding, "Estimating the parameters of the K distribution in the intensity domain," Defence Sci. Technol. Org., Salisbury, SA, Australia, Tech. Rep. DSTO-TR-0839, Jul. 1999.

[46] C. Walck, "Hand-book on statistical distributions for experimentalists," Stockholm Univ., Stockholm, Sweden, Tech. Rep. SUF–PFY/96–01, Sep. 2007.

[47] S. Kotz, T. J. Kozubowski, and K. Podgorski, *The Laplace Distribution and Generalizations: A Revisit With Applications to Communications, Economics, Engineering and Finance*. New York, NY, USA: Springer, 2001.

[48] L. Leemis. (May 2012). *Univariate Distribution Relationships*. [Online]. Available: http://www.math.wm.edu/~leemis/chart/UDR/PDFs/ExponentialLaplace.pdf

[49] J. G. Proakis, *Digital Communications*, 4th ed. Boston, MA, USA: McGraw-Hill, 2001.

[50] N. P. Le, L. C. Tran, F. Safaei, and V. S. Varma, "Energy efficiency analysis of antenna selection MIMO ARQ systems over Nakagami-m fading channels," *IET Commun.*, vol. 9, no. 12, pp. 1522–1530, 2015.

[51] N. P. Le, L. C. Tran, and F. Safaei, "Optimal design for energy-efficient per-subcarrier antenna selection MIMO-OFDM wireless systems," *Wireless Pers. Commun.*, vol. 84, no. 4, pp. 3001–3014, Apr. 2015.

[52] N. P. Le, F. Safaei, and L. C. Tran, "Antenna selection strategies for MIMO-OFDM wireless systems: An energy efficiency perspective," *IEEE Trans. Veh. Technol.*, vol. 65, no. 4, pp. 2048–2062, Apr. 2016.

[53] S. Cui, A. J. Goldsmith, and A. Bahai, "Energy-constrained modulation optimization," *IEEE Trans. Wireless Commun.*, vol. 4, no. 5, pp. 2349–2360, Sep. 2005.

[54] B. Van Der Doorn, W. Kavelaars, and K. Langendoen, "A prototype low-cost wakeup radio for the 868 MHz band," *Int. J. Sensor Netw.*, vol. 5, no. 1, pp. 22–32, Feb. 2009.

[55] S. Marinkovic and E. Popovici, "Nano-power wake-up radio circuit for wireless body area networks," in *Proc. IEEE Radio Wireless Symp. (RWS)*, Jan. 2011, pp. 398–401.

[56] R. D'Errico and L. Ouvry, "Time-variant BAN channel characterization," in *Proc. 20th IEEE Int. Symp. Pers., Indoor Mobile Radio Commun. (PIMRC)*, 2009, pp. 3000–3004.

Le Chung Tran (M'09) received the B.E. degree (Hons.) from the University of Communication and Transport, in 1997, the M.E. degree from the University of Science and Technology, Vietnam, in 2000, and the Ph.D. degree from the University of Wollongong (UOW), Australia, in 2006, respectively, all in telecommunications engineering. Before joining UOW, he had been a Lecturer with the University of Communication and Transport, Vietnam, since 1997. From 2005 to 2006, he was an Associate Research Fellow with the Wireless Technologies Laboratory, UOW. From 2006 to 2008, he was a Post-Doctoral Research Fellow with the University of Lübeck, Germany, under the Alexander von Humboldt Fellowship. He has been with the UOW since 2009, where he is currently a Senior Lecturer. He has achieved the World University Services Award twice, the Vietnamese Government's Doctoral Scholarship, the International Postgraduate Research Scholarship, and the prestigious Humboldt Post-Doctoral Fellowship. He has been an Editorial Board Member of the *Electrical Engineering: An International Journal*, an organizing committee member (Track Chair, Session Chair, Publicity Co-Chair), and a Technical Program Committee (TPC) member of 29 IEEE conferences. He is a co-author of over 60 publications, including one book, which is hold in 337 worldwide libraries. His research interests include 5G, multiple-input multiple-output, ultra-wideband, space-time-frequency processing, cooperative and cognitive communications, software defined radio, network coding, full duplex communications, wireless body area networks, and digital signal processing for communications.

Alfred Mertins (M'96–SM'03) received the Dipl.-Ing. degree in electrical engineering from the University of Paderborn, Paderborn, Germany, in 1984, and the Dr.-Ing. degree in electrical engineering from the Hamburg University of Technology, Hamburg, Germany, in 1991. From 1986 to 1991, he was a Research Assistant with the Hamburg University of Technology, and from 1991 to 1995, he was a Senior Scientist with the Microelectronics Applications Center, Hamburg. From 1996 to 1997, he was with the University of Kiel, Kiel, Germany, and from 1997 to 1998, he was with the University of Western Australia, Perth. In 1998, he joined the University of Wollongong, where he was an Associate Professor of Electrical Engineering. From 2003 to 2006, he was a Professor with the Faculty of Mathematics and Science, University of Oldenburg, Germany. In 2006, he joined the University of Lübeck, Lübeck, Germany, where he is currently a Professor and the Director of the Institute for Signal Processing. His research interests include speech, audio, and image processing, wavelets and filter banks, pattern recognition, and digital communications.

Xiaojing Huang (M'99–SM'11) received the B.E., M.E., and Ph.D. degrees from Shanghai Jiao Tong University, Shanghai, China, in 1983, 1986, and 1989, respectively, all in electronic engineering. He is currently a Professor of Information and Communications Technology with the School of Computing and Communications and the Program Leader for mobile sensing and communications with the Global Big Data Technologies Center, University of Technology Sydney, Australia. He had been a Principal Research Scientist with Commonwealth Scientific and Industrial Research Organization (CSIRO), Australia, and the Project Leader of CSIRO microwave and mm-wave backhaul projects since 2009, an Associate Professor with the University of Wollongong, Australia, since 2004, and a Principal Research Engineer with the Motorola Australian Research Center since 1998. With over 27 years of combined industrial, academic, and scientific research experience, he has authored over 250 book chapters, refereed journal and conference papers, and major commercial research reports. He has also filed 29 patents. He was a recipient of the CSIRO Chairman's Medal and the Australian Engineering Innovation Award in 2012 for exceptional research achievements in multigigabit wireless communications.

Farzad Safaei (M'97–SM'14) B.E. degree in electronics from the University of Western Australia, and the Ph.D. degree in telecommunications engineering from Monash University in 1998. He was the Manager of Internetworking Architecture and Services Section, Telstra Research Laboratories. He was the Managing Director of ICT Research Institute, from 2008 to 2013 and the Program Director of the Smart Services Cooperative Research Center, Australia from 2007 to 2014. He is currently the Chair of Telecommunications Engineering with the University of Wollongong. His main research interests include multimedia signal processing and communications technology. He is the winner of a number of awards, including the top Australian and Asia Pacific Awards for ICT Research and Development in 2012.